
Article:
Chen, Q, Zafar, U, Ghadiri, M orcid.org/0000-0003-0479-2845 et al. (1 more author) (2017) Assessment of Surface Caking of Powders Using the Ball Indentation Method. International Journal of Pharmaceutics, 521 (1-2). pp. 61-68. ISSN 0378-5173

https://doi.org/10.1016/j.ijpharm.2017.02.033

Title: Assessment of Surface Caking of Powders Using the Ball Indentation Method

Authors: Qinqin Chen, Umair Zafar, Mojtaba Ghadiri, Jinfeng Bi

PII: S0378-5173(17)30114-X
DOI: http://dx.doi.org/doi:10.1016/j.ijpharm.2017.02.033
Reference: IJP 16437

To appear in: *International Journal of Pharmaceutics*

Received date: 27-11-2016
Revised date: 12-2-2017
Accepted date: 13-2-2017

Please cite this article as: Chen, Qinqin, Zafar, Umair, Ghadiri, Mojtaba, Bi, Jinfeng, Assessment of Surface Caking of Powders Using the Ball Indentation Method.International Journal of Pharmaceutics http://dx.doi.org/10.1016/j.ijpharm.2017.02.033

Assessment of Surface Caking of Powders Using the Ball Indentation Method

Qinqin Chen[1,2], **Umair Zafar**[2], **Mojtaba Ghadiri**[2,*] m.ghadiri@leeds.ac.uk , **Jinfeng Bi**[1]

[1]*Institute of Food Science and Technology, Chinese Academy of Agricultural Science (CAAS)/ Key Laboratory of Agro-Products Processing, Ministry of Agriculture, Beijing 100193, China*

[2]*School of Chemical and Process Engineering, University of Leeds, Leeds LS2 9JT, UK*

[*]Corresponding author: Tel.: +44 (0)113 3432406

Graphical abstract

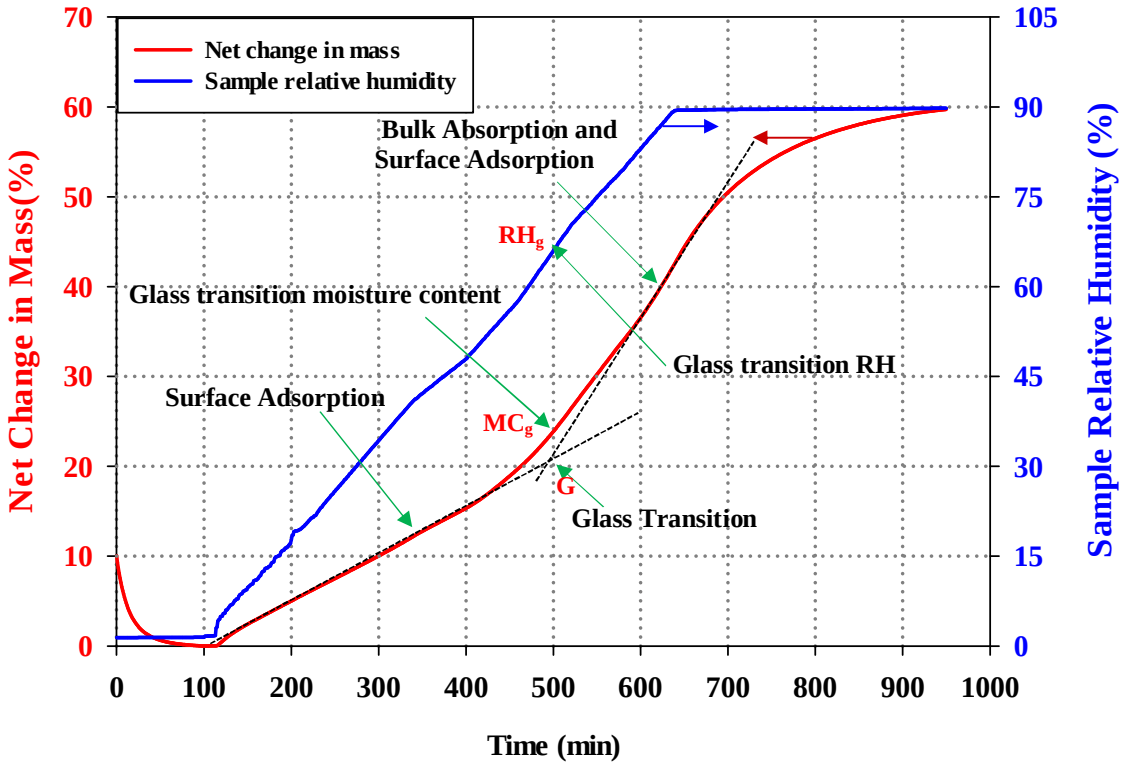

Highlights

- Relative humidity and temperature show coupled effect on powder surface caking.
- Irreversible caking is formed in PVP and HPC at 75% relative humidity (RH).
- The critical glass transition RH for PVP at 25 ℃ and 45℃ are 63% and 53%.
- The critical glass transition RH for HPC at 25 ℃ and 45℃ are 61% and 50%.
- Ball indentation is an effective method for assessment of powder surface caking.

Abstract

Powder caking is a ubiquitous problem, which could significantly decrease product quality and lead to economic losses. Hence it is important to know the conditions under which it occurs. The caking behaviour of three powder materials (PVP, HPC and $CaHPO_4$) has been investigated by the ball indentation method (BIM) as affected by relative humidity (RH), temperature and time. The resistance to powder flow, as indicated by the hardness is measured by a ball indenting the powder bed surface. The surface hardness increases with increasing RH and temperature, indicating caking of the powder bed. Moreover, the temperature and RH show a coupled effect on powder caking. Irreversible caking is formed in PVP and HPC at 75% RH; the particles coalesce and the volume of powder bed is significantly reduced with time. However, the caking of $CaHPO_4$ is reversible. To examine the caking mechanism of PVP and HPC, the critical glass transition RH is determined at 25 °C and 45 °C. The values are 63% and 53% RH for PVP and 61% and 50% RH for HPC, respectively. The glass transition moisture content in the ball indentation experiments is comparable with that determined by the dynamic vapor sorption measurement. BIM could be a fast and effective method for the assessment of powder surface caking.

Keywords: pharmaceutical powders, ball indentation, caking, moisture sorption, hardness, glass transition

1. Introduction

Caking is deleterious in powder processing operations. It transforms the powder into lumps, agglomerated solid or sticky material (Aguilera *et al.,* 1995). Caked powders cause processing difficulties and lower the quality of the final products, hence leading to downtime and significant economic losses (Carpin *et al.,* 2016; Aguilera *et al.,* 1995). It is therefore of great importance to know the conditions under which powders are prone to caking and how to mitigate it.

Caking of powders is influenced by a large number of factors: particle size, shape, relative humidity, temperature, applied force, hygroscopicity, deliquescence and possible solid state transformations. Hence, it is difficult to predict the caking affinity of any powder (Carpin *et al.,* 2016). Several methods are used nowadays to characterise caking, including the uniaxial compression test (Chávez Montes *et al.,* 2011), powder rheometer (Freeman *et al.,* 2015), environmentally controlled caking rig (Calvert *et al.,* 2013),

Edinburgh powder tester (Thakur *et al.,* 2014), shear cell (Cleaver *et al.*, 2004), and caking index test (Irani *et al.,* 1959). A comprehensive review of caking and methods for its characterisation have recently been made by Zafar *et al.* (2017b). When the interest is on a small quantity of powders at very low stress levels, the Ball Indentation Method (BIM), developed by Hassanpour and Ghadiri (2007) can detect the surface caking of the powders very quickly with high sensitivity. It assesses the resistance of the powder bed to plastic deformation using a simple mechanical testing machine. It has been used recently to characterise the flowability of cohesive powders (Pasha *et al.,* 2013; Zafar *et al.,* 2015; Zafar *et al.,* 2017a). In this work we expand its application for assessing the onset of powder caking.

During handling, storage, processing and distribution, powders may experience variations in temperature and humidity, which are key causes of powder caking (Fitzpatrick *et al.,* 2010). The glass transition of powders, which have amorphous content, would occur when they are exposed to a high relative humidity or temperature (Carpin *et al.,* 2016; Fitzpatrick *et al.,* 2010). It is thus important to know the moisture and temperature sensitivities of powders for predicting caking. In the present study, three pharmaceutical excipient powders with different hygroscopicity are used. Effects of relative humidity and temperature on their surface caking behaviour are examined by BIM. A lightly compacted powder bed in a die is exposed to environment conditions with different relative humidity and temperature values for different periods of time. The caking behaviour is then analysed in terms of the glass transition RH and temperature.

2. Materials and Methods

Povidone (PVP, grade: Kollidon 30), Hydroxypropyl Cellulose (HPC, grade: KLUCEL EXF), calcium phosphate dibasic anhydrous ($CaHPO_4$, grade: A-TAB) are widely used in pharmaceutical industry. They are prone to caking, hence they were selected for this work. Samples of powders were provided by AstraZeneca Ltd (Macclesfield, UK). To obtain different relative humidity levels (11%, 33%, 75%), lithium chloride (LiCl, purity > 99%), magnesium chloride ($MgCl_2$, purity > 98%), and sodium chloride (NaCl, purity > 99.5%) were used to prepare saturated salt solutions with which the powders were conditioned. They were all of analytical grade, and were obtained by Fisher Scientific UK Ltd (Loughborough, UK).

Morphologi G3 (Malvern Instruments Ltd, Worcestershire, UK) was used for particle size and shape analyses. The dry sample dispersion unit (SDU) was used and a sample of about 3 mm^3 was dispersed onto a glass plate using 1 bar injection pressure, injection time of 20 ms, and settling time of 60 s. The projected area of particles was determined by automatic image analysis and the results are expressed as circle equivalent (CE) diameter, presented on the volume distribution. The characteristic particle sizes for the cumulative distribution at 10%, 50% and 90% undersize (CE $D_{[v,0.1]}$, CE $D_{[v,0.5]}$, and CE $D_{[v,0.9}$) are reported, together with circularity, aspect ratio and elongation in Table 1. $CaHPO_4$ has the widest size distribution and the largest average size (CE $D_{[v,0.5]}$=197 µm), however, there is no significant difference of size distribution between PVP and HPC. PVP has the highest value of circularity (0.969), HPC exhibits the highest value of elongation and lowest value of aspect ratio, owing to its fibrous structure.

The images of the particles were viewed with a TM3030Plus table-top scanning electron microscope (Hitachi High-Technologies Corporation, Tokyo, Japan) and are shown in Figure 1. PVP is more spherical, however, there are many dents on its surface (Figure 1 (a)). HPC has a fibrous type profile with a very irregular shape (Figure 1 (b)), while $CaHPO_4$ shows a crystal structure (Figure 1 (c)).

The moisture sorption behaviour of the powders was determined with a dynamic vapour sorption analyser (DVS) (Surface Measurement Systems Ltd., London, UK) equipped with a Cahn microbalance. The experiments were carried out at 25 °C and 45 °C with different relative humidity levels (RH) ranging from 0% to 90%. Approximately 10 mg of powders was loaded onto the sample pan. Initially, the samples were dehydrated in the DVS chamber at 0% RH until the equilibrium mass was obtained. The samples were then subjected to hydration with 10% RH steps. The value of dm/dt (m: mass of sample; t: time) was set to be below 0.002 %/min. Each experiment was performed in three repeats. The moisture uptakes of PVP, HPC and $CaHPO_4$ as a function of relative humidity at 25 °C and 45 °C are shown in Figure 2. PVP, HPC and $CaHPO_4$ present high, medium and low moisture sorption behaviour, having moisture content of 57.46%, 21.44% and 3.16%, respectively, at 90% RH and 25 °C. Temperature shows a significant effect on the moisture sorption behaviour of the powders. For all the samples, the moisture uptake at a particular RH decreases with increasing temperature. At 90% RH, the moisture contents of PVP, HPC and $CaHPO_4$ at 45 °C are 77%, 67% and 60% of those at 25 °C, respectively. At higher temperatures, the attractive forces between the water molecules of solid surfaces decrease due to the increase in the kinetic energy of

water molecules. Hence, the water molecules are bound more easily to binding sites on the surface of powders at low temperatures (Djendoubi Mrad *et al.*, 2013).

Powder flow behaviour was analysed using the Schulze RST-XS annular ring shear cell tester (Wolfenbüttel, Germany). The applied pre-shear normal stresses (σ_{pre}) were 2, 4, and 6 kPa. For each σ_{pre}, five shear stresses were used to construct a yield locus following the standard procedure (Schulze, 2008), from which the "flowability index (*ffc*)", the ratio of the major principal stress (σ_1) to the unconfined yield strength (σ_c), was determined (Schulze and Wittmaier, 2003). The lowest normal stress was kept at 1 kPa, while other points were equally distributed. The results are given in Figure 3. Each point is the average values of three repeats. For all the pre-shear normal stresses tested, the resulting flowability index for both HPC and $CaHPO_4$ are found to fall within the regime of 'very cohesive and 'free flowing', respectively. However, for the case of PVP, a change of flowability regime from 'easy flowing' to 'free flowing' is observed when the pre-shear normal stress is increased from 2 to 4 kPa. Flowabilities of the three samples are in the order: $CaHPO_4$ >PVP > HPC.

Surface caking was characterised by BIM. Samples were consolidated into a cylinder (40 mm diameter) by a stainless steel piston using an Instron 5566 series mechanical testing machine (Instron European Headquarters, Buckinghamshire, UK) at the consolidation pressure of 7.5 kPa. They were then subjected to indentation using a glass spherical indenter with the diameter of 3.969 mm (Sigmund Lindner GmbH, Warmensteinach, Germany). The loading speed was 1mm/min. During the ball indentation process, the applied load (F) and the displacement of the indenter were continuously recorded, and a typical example of indentation loading/unloading cycle on HPC powder bed is shown in Figure 4.

The resistance to plastic deformation of the bulk powder (expressed by the hardness) is used to evaluate the surface caking of powder bed. The hardness (*H*) of a consolidated powder bed could be calculated by (Hassanpour and Ghadiri, 2007):

$$H=F_{max}/\pi\,(D_b\times h_{c,max}-h^2_{c,max}) \qquad (1)$$

where F_{max} is the maximum indentation load, D_b is the diameter of the indenter, and $h_{c,max}$ is the intercept of the tangent to the unloading curve, as shown in Figure 4.

Effects of the relative humidity (RH) and temperature on the surface powder caking were investigated by BIM. The tests are done by exposing a compacted powder bed in a die to a certain environment with three different relative humidity levels and two temperatures for a number of days based on the caking kinetics. Similar to the moisture sorption experiments, the low (11%), medium (33%) and high (75%) relative humidity levels were created by the saturated salt solutions of LiCl, $MgCl_2$ and NaCl, respectively, and two temperatures of 25 °C and 45 °C were used. The indentation tests were also carried out in three repeats.

The relative humidity at which the glass transition occurred was determined by DVS for PVP and HPC powders. Approximately 10 mg of powders was used and initially dried at 0% RH. They were then exposed to a linearly increasing RH from 0 to 90% RH with ramping rates of 2%, 6% and 10% RH/hour, respectively. The glass transition RH was considered as the inflection point between surface adsorption and bulk absorption (Burnett *et al*., 2004). These experiments were also carried out at 25 °C and 45 °C in triplicate tests.

3. Results and Discussion

3.1 Assessment of powder surface caking by Ball Indentation Method

The powder bed was pre-consolidated at 7.5 kPa (9.42 N load). The effects of indentation load and position on the hardness of different powder beds were first investigated. After suitable conditions of indentation load and position were confirmed, the effects of relative humidity and temperature on the caking of powder were further studied.

3.1.1 Effect of indentation load and position on the hardness of powder bed

To investigate the effect of indentation load on hardness measurement by BIM, different indentation loads were used for different samples (3-11mN for PVP, 10-200 mN for HPC, 3-20 mN for $CaHPO_4$) and the results are shown in Figure 5(a). The distance between the indenter and die wall (D_{iw}) was 8 mm, while the distance between two successive indentations (D_{ii}) was 11 mm (Figure 6 (a)).

In the ball indentation test, the hardness is inferred from the relationship between the penetration depth and the force acting on the indenter (Zafar *et al*., 2017a). The dimensionless penetration depth (h_d), which is calculated by the penetration depth ($h_{c,max}$) divided by the radius of the indenter (R_i), is used as the independent variable. Hardness should be independent of penetration depth and indentation load when the

bulk powder undergoes plastic deformation. PVP and $CaHPO_4$ show similar results. Their hardness values are relatively stable around 0.8 and 1.6 kPa, respectively, under different indentation loads (Figure 5(a)). However, for HPC lower values of hardness are obtained at very low penetration depths. When the indentation load is over 100 mN, the hardness values of HPC become stable (about 17 kPa). Hence, it is very important to have enough indentation loads to get a reliable hardness measurement. Based on the previous study, the dimensionless penetration depth should be more than 0.4 to give a reliable measure of the hardness (Zafar *et al*., 2017a). Therefore, the indentation loads 7, 15, 150 mN were used for PVP, $CaHPO_4$ and HPC tests in the following study, respectively.

The effect of indentation position on material hardness was investigated and the results are shown in Figure 5 (b). Eight indentations were carried out on the same powder bed, the values of D_{iw} and D_{ii} were 8 and 9 mm, respectively (Figure 6 (b)). At the indentation loads of 7, 15, and 150 mN, the hardness values of PVP, $CaHPO_4$ and HPC are in the range 0.81-0.95, 1.48-1.80 and 14.2-19.2 kPa, respectively. The average hardness values of PVP, $CaHPO_4$ and HPC for the eight indentation positions are 0.87 ±0.05, 1.65±0.09, 16.50 ± 1.7 kPa, respectively. Although there was some fluctuation in the value of hardness in different positions, the results were relatively stable for different samples. Therefore, eight positions could be used on one die in the further dynamic study.

3.1.2 Effect of relative humidity on the surface caking of powders

Powders were exposed to 11%, 33% and 75% RH at 25 °C for 8 days, the changes of the bed surface hardness are shown in Figure 7. When PVP was exposed to 11% RH, the hardness of the powder bed surface at different times had no significant change (Figure 7(a)). For 33% RH, the powder bed surface hardness of PVP increased slightly and approached a plateau of around 3kPa in six days. However, there was a substantial increase in hardness of PVP at 75% RH. The hardness value was the highest (2118 kPa) at 7-day exposure to 75% RH, which was 2500 times of that of the start of exposure (0-day). The colour of PVP changed from light yellow to yellow; the powder had visually transformed from a powder into a solid material. In the cases of HPC and $CaHPO_4$, the low (11%) and medium (33%) RH did not show a significant effect on the hardness of powder beds. However, the hardness of both powder beds significantly increased at 75% RH. The volume of HPC powder bed started to reduce after 3-day exposure. The change of hardness of $CaHPO_4$ was smaller than that of the others, it approached a plateau at day 5 (3.59 kPa), which was less than twice the value of day 0. The powder cake was very weak and easily broke down.

After 8-day exposure to 75% RH, the hardness of PVP was the highest, followed by HPC and $CaHPO_4$, with the latter showing the lowest. The trend is related to the moisture sorption behaviour which is shown in Figure 2 and is further analysed below.

3.1.3 Effect of temperature on the surface caking of powders

The experiments were carried out at 25 °C and 45 °C under 75% RH; the results are shown in Figure 8. The hardness values are much larger at 45 °C than those at 25 °C, particularly for PVP and to a lesser extent for HPC, but the changes are still orders of magnitude, even though there is less moisture sorption at the higher temperature (Figure 2). This implies that temperature and relative humidity have a coupled effect on powder caking. When PVP is exposed at 45 °C to 75% RH, the hardness value increases first and reaches the highest value at 2-day with a value of almost 13 MPa. Then it decreases significantly by an order of magnitude with time. The states of the PVP powder beds at 45 °C and 25 °C after 8-day exposure to 75% RH are very different. The particles are regarded as "transformed" at the higher temperature, whilst they are simply "bonded" at the lower temperature (Oksanen and Zografi, 1990). For HPC and $CaHPO_4$, the hardness of both samples increases with temperature, albeit to a minor extent for the latter. The hardness of HPC after 1-day exposure to 45 °C is similar to that of 8-day exposure to 25 °C. Clearly high temperatures could significantly accelerate the caking rate of powders. After 8-day exposure to 75% RH, the hardness of HPC at 45 °C is six times that of 25 °C. More particles are bonded together at the higher temperature, hence, the volume of powder bed decreases. However, the powder cake of $CaHPO_4$ is still very weak, even after 8-day exposure to 45 °C and 75% RH, where its hardness is only 7.68 kPa. The caking of $CaHPO_4$ is reversible, presumably due to its very low moisture sorption ability (about 1%), a strong cake cannot form even at the high temperature and relative humidity (Figure 2). Clearly $CaHPO_4$ has a good stability and not prone to caking.

3.2 Caking mechanism of PVP and HPC

Significant caking occurs in PVP and HPC powders at high RH and temperatures. The degree of caking is related to the moisture uptake and glass transition. To interpret the caking behaviour of PVP and HPC which are amorphous, the relative humidity corresponding to the glass transition is examined at 25 °C and 45°C.

A typical net change in mass (based on dry basis) versus time for PVP at 25 °C with RH ramping rate of 10% RH/h is displayed in Figure 9. The water uptake is relatively low and increases linearly with RH below 40%. The moisture uptake in this region is mainly dominated by the surface adsorption of water. With RH increasing further, there is a sharp increase in moisture uptake. This has been attributed to the bulk absorption of water by PVP (Burnett *et al.*, 2004). The glass transition relative humidity (RH_g) is inferred from the transition point between surface adsorption to bulk absorption (Figure 9**,** about 500 min and 67% RH); the glass transition moisture content (MC_g) is determined as 24%. This value is obviously dependent on the rate of increase of RH. Similar experiments have also been done at 2% and 6% RH/h. The ramping rates and corresponding RH_g and MC_g values are shown in Figure 10.

As Figure 10 (a) indicates, RH_g decreases with decreasing ramping rate. Meanwhile, there seems to be linear relationships between RH ramping rate and RH_g at 25 °C and 45 °C with correlation coefficients (R^2) better than 0.95. The critical RH_g is calculated by extrapolating the results to zero ramping rate. It decreases with the increase of temperature. The critical RH_g values for PVP at 25 °C and 45 °C are 63% and 53% RH, respectively. Therefore the glass transition of PVP readily occurs on exposure to 75% RH. Similarly, a linear fit appears to prevail between the ramping rate and MC_g values (R^2>0.95). The critical MC_g for PVP at 25 °C and 45 °C are 22.86 % and 14.13 %, respectively (Figure 10 (b)).

To explore the significance of the results, the change of moisture uptake and hardness of PVP are shown together in Figure 11. There are turning points in changes of hardness with time at 25 °C and 45 °C (at 7-day and 2-day, respectively). After that, the hardness decreases due to deliquescence with more moisture uptake, resulting in a decrease in the powder bed volume. The powder bed is transformed from a solid glassy state into a highly viscous rubbery state; the particles agglomerate first and eventually coalesce with each other (Fitzpatrick *et al.*, 2010). The state of PVP is therefore changed from “bonded” to “transformed”. The onset of glass transition of PVP is considered as 7-day and 2-day for exposure to 75% RH at 25 °C and 45 °C, respectively. The corresponding moisture contents of PVP are 22.89 % and 14.51 %, respectively, which is comparable with the critical MC_g value predicted above.

Similar experiments have also been performed on HPC powder at 2%, 6%, and 10% RH/h and 25 °C and 45 °C. RH_g and MC_g values of HPC as a function of the ramping rate are shown in Figure 12. The RH_g values plotted versus ramping rate for the two temperatures also indicate a linear correlation (R^2>0.96). The critical RH_g values of HPC at 25 °C and 45 °C are 61% and 50% RH, respectively. RH_g increases with

increasing ramping rate. However, the ramping rate shows more effect on the RH_g values of HPC than PVP. When the ramping rate is decreased from 10% to 2% RH/h at 25 ℃, the RH_g value differences [$RH_{g,\ 10\%RH/h}$ - $RH_{g,\ 2\%RH/h}$] of HPC and PVP are 8.29% and 3.78%, respectively (Figure 12 (a)). However, the differences of RH_g value [$RH_{g,\ 10\%RH/h}$ - $RH_{g,\ 2\%RH/h}$] of HPC and PVP are significantly increased at 45 °C to 14.7% and 11.2 % when the ramping rate is decreased from 10% to 2% RH/h. As Figure 12 (b) indicates, MC_g decreases with the increase of temperature. The critical MC_g values of HPC at 25 ℃ and 45 °C are 6.05 % and 3.59 %, respectively. Molecular mobility increases with temperature, hence the glass transition is induced by less water uptake (Burnett *et al.*, 2004). The changes of moisture uptake and hardness of HPC are shown in Figure 13. Visual observations of the HPC bed surface show the bed volume decreasing with time; after exposure for durations of 3-day at 25 °C or 1-day at 45 °C to 75% RH the bed detaches itself from the containing wall with a clear visible gap, indicating the occurrence of glass transition. At these points in time the corresponding moisture contents are 7.07 % and 5.45 %, respectively, which are a little higher than the critical MC_g values predicted above (6.05 % and 3.59 %).

4. Conclusions

An assessment of surface caking of PVP, HPC and $CaHPO_4$ powders has been made by BIM. The hardness of powder beds of PVP, HPC and $CaHPO_4$ increases with increasing RH and temperature. RH and temperature show a coupled effect on the caking of powders. Strong cakes are formed for PVP and HPC at 75% RH; In contrast, the cake of $CaHPO_4$ is very weak and easily breaks down. The glass transition of PVP occurs when the RH is over 63% and 53% RH at 25 °C and 45 °C, respectively. The state of the powder bed of PVP changes from “bonded” to “transformed” on adsorption of moisture and undergoes deliquescence. Once the RH of HPC is increased beyond 61% and 50% RH at 25 °C and 45 °C, respectively, samples transform from a glassy state into a rubbery state; particles fuse together and the volume of the powder bed decreases significantly. The moisture content at which the glass transition occurs (MC_g) is detected by the hardness of the powder bed surface. It turns out the MC_g values are comparable with the critical MC_g values predicted by DVS measurements. The results indicate that BIM is a fast, effective and reliable method for assessing powder surface caking.

Acknowledgements

The authors are thankful to Dr David Wilson (AstraZeneca, Macclesfield, UK) for his support and providing the raw material required for the research. The financial support of China Scholarship Council (No. 201503250016) for the first author is gratefully acknowledged.

REFERENCES

Aguilera, J., del Valle, J., Karel, M.,;1; 1995. Caking phenomena in amorphous food powders. *Trends Food Sci. Technol.* 6(5), 149–155.

Burnett, D.J., Thielmann, F., Booth, J.,;1; 2004. Determining the critical relative humidity for moisture-induced phase transitions. *Int. J. Pharm.* 287(1–2), 123–133.

Calvert, G., Curcic, N., Redhead, C., Ahmadian, H., Owen, C., Beckett, D., Ghadiri, M. ;1;2013.A new environmental bulk powder caking tester. *Powder Technol.* 249, 323–329.

Carpin, M., Bertelsen, H., Bech, J. K., Jeantet, R., Risbo, J., Schuck, P.;1; 2016. Caking of lactose: A critical review. *Trends Food Sci. Technol.* 53, 1–12.

Chávez Montes, E., Ardila Santamaría, N., Gumy, J. C., Marchal, P.;1; 2011. Moisture-induced caking of beverage powders. *J. Sci. Food Agric.* 91(14), 2582–2586.

Cleaver, J. A. S., Karatzas, G., Louis, S., Hayati, I.;1; 2004. Moisture-induced caking of boric acid powder. *Powder Technol.*146(1–2), 93–101.

Djendoubi Mrad, N., Bonazzi, C., Courtois, F., Kechaou, N., Boudhrioua Mihoubi, N.;1; 2013. Moisture desorption isotherms and glass transition temperatures of osmo-dehydrated apple and pear. *Food Bioprod. Process.* 91(2), 121–128.

Fitzpatrick, J. J., Descamps, N., O'Meara, K., Jones, C., Walsh, D., Spitere, M.;1; 2010. Comparing the caking behaviours of skim milk powder, amorphous maltodextrin and crystalline common salt. *Powder Technol.* 204(1), 131–137.

Freeman, T., Brockbank, K., Armstrong, B.;1;, 2015. Measurement and quantification of caking in powders. *Procedia Eng.* 102, 35–44.

Hassanpour, A., Ghadiri, M.,;1; 2007. Characterisation of flowability of loosely compacted cohesive powders by indentation. *Part. Part. Syst. Charact.* 24(2), 117–123.

Irani, R.R., Callis, C.F., Liu, T., ;1;1959. How to select flow conditioning and anticaking agents. *Ind. Eng. Chem.* 51(10), 1285–1288.

Oksanen, C. A., Zografi, G., ;1;1990. The relationship between the glass transition temperature and water vapor absorption by poly(vinylpyrrolidone). *Pharm. Res.* 7(6), 654–657.

Pasha, M., Hare, C., Hassanpour, A., Ghadiri, M.;1; 2013. Analysis of ball indentation on cohesive powder beds using distinct element modelling. *Powder Technol*. 233, 80–90.

Schulze, D., Wittmaier, A.,;1; 2003. Flow properties of highly dispersed powders at very small consolidation stresses. *Chem. Eng. Technol*. 26, 133–137.

Schulze, D.;1;, 2008. 6 Discussion of testers and test procedures. In *Powders and Bulk Solids*. Berlin, Heidelberg: Springer Berlin Heidelberg, 163–198.

Thakur, S.C., Ahmadian, H., Sun, J., Ooi, J. Y.;1; 2014. An experimental and numerical study of packing, compression, and caking behaviour of detergent powders. *Particuology* 12(1), 2–12.

Zafar, U., Hare, C., Calvert, G., Ghadiri, M., Girimonte, R., Formisani, B., Quintanilla, M.A.S., Valverde, J. M. ;1;2015. Comparison of cohesive powder flowability measured by Schulze Shear Cell, Raining Bed Method, Sevilla Powder Tester and new Ball Indentation Method. *Powder Technol.* 286, 807–816.

Zafar, U., Hare, C., Hassanpour, A., Ghadiri, M. ;1;2017a. Ball indentation on powder beds for assessing powder flowability: Analysis of operation window. *Powder Technol*. 310, 300-306.

Zafar U., Vivacqua V., Calvert G., Ghadiri M., Cleaver J.A.S.;1; 2017b. A Review of Bulk Powder Caking. *Powder Technol*. POWTEC-D-16-02232.

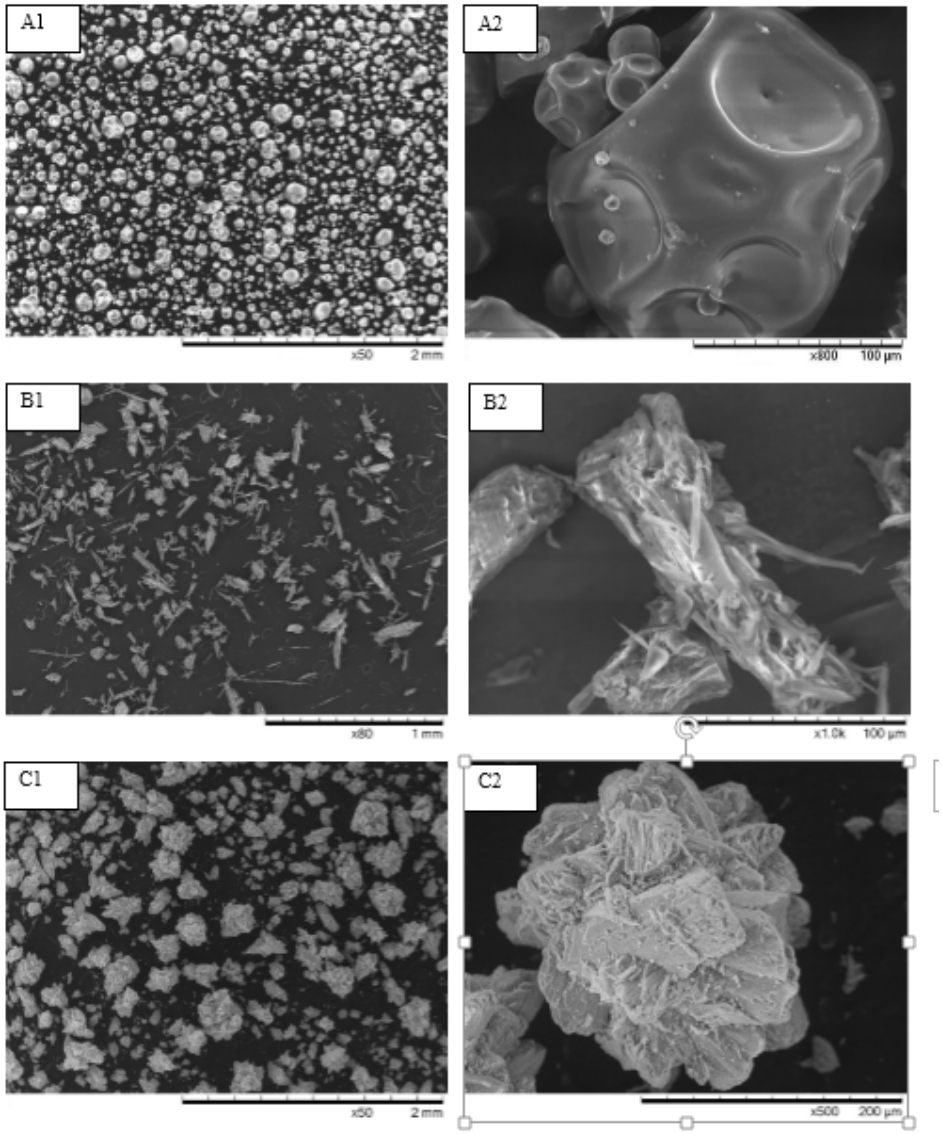

Figure Captions:

Figure 1. SEM of PVP (A1: 50×; A2: 800×), HPC (B1: 80×; B2: 1000×),) and $CaHPO_4$ (C1: 50×; C2: 500×)

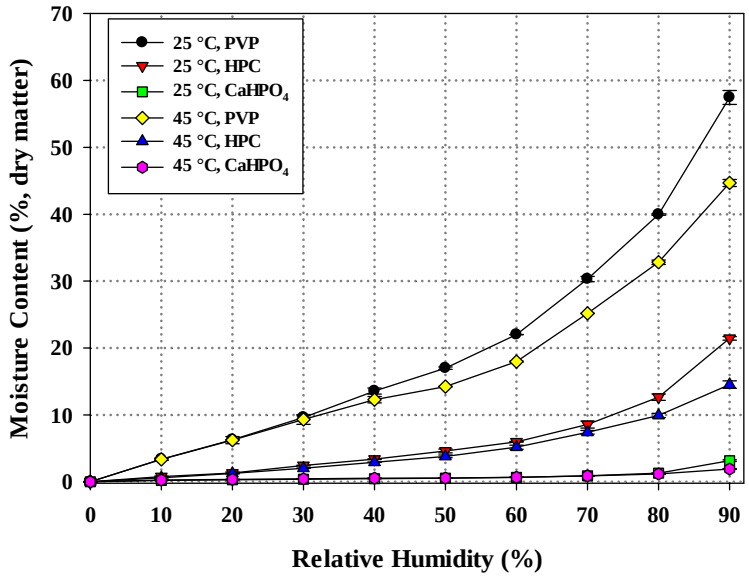

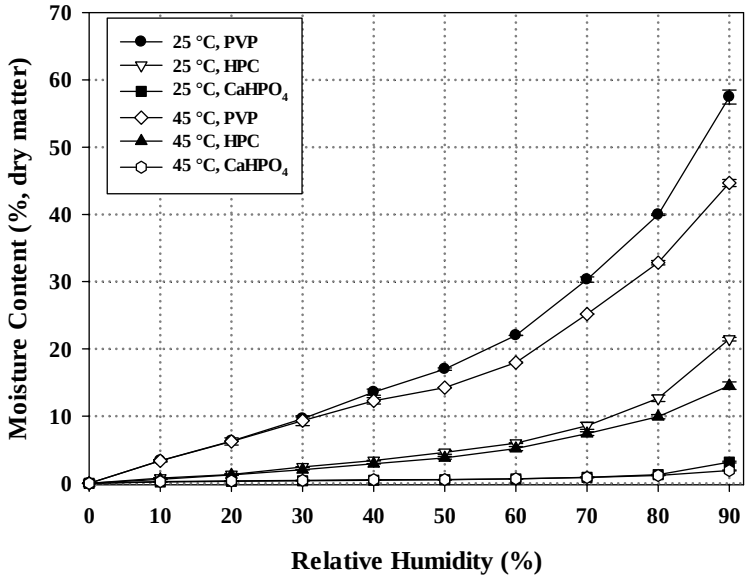

Figure 2. Moisture sorption behaviours of PVP, HPC, and $CaHPO_4$ at 25°C and 45°C

Figure 3 (Colour; Black and white)

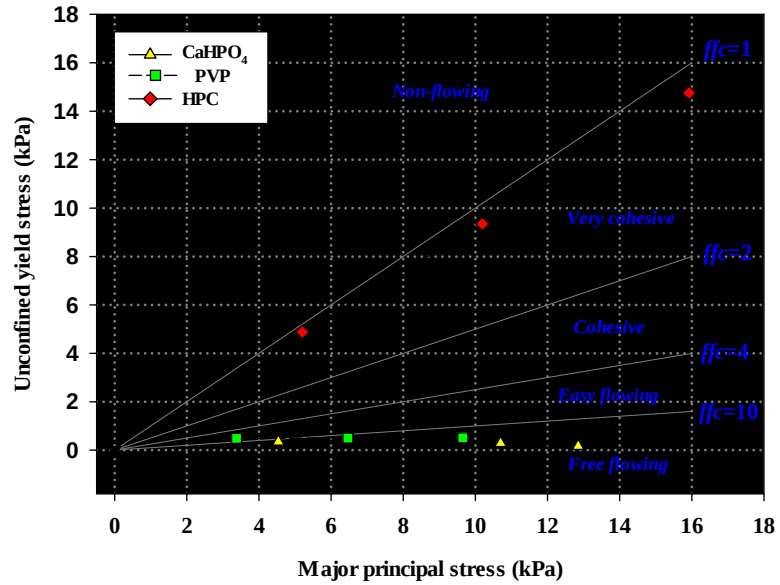

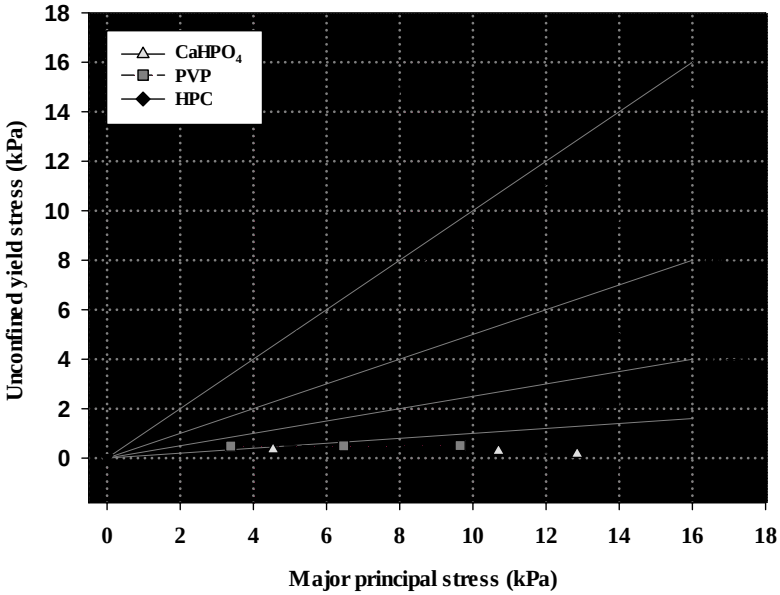

Figure 3. Flow functions of PVP, HPC, and $CaHPO_4$ at different pre-shear normal stresses

Figure 4 (Colour; Black and white)

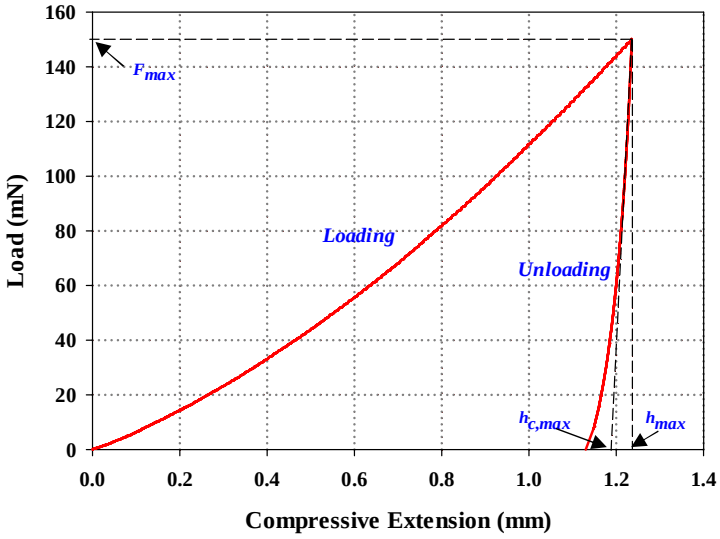

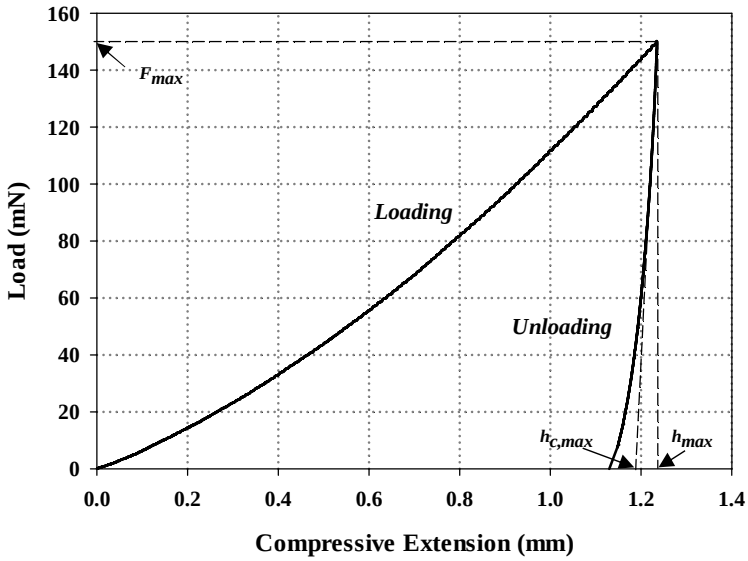

Figure 4. A typical loading/unloading curve of the ball indentation process on the HPC powder bed

Figure 5 a) (Colour; Black and white)

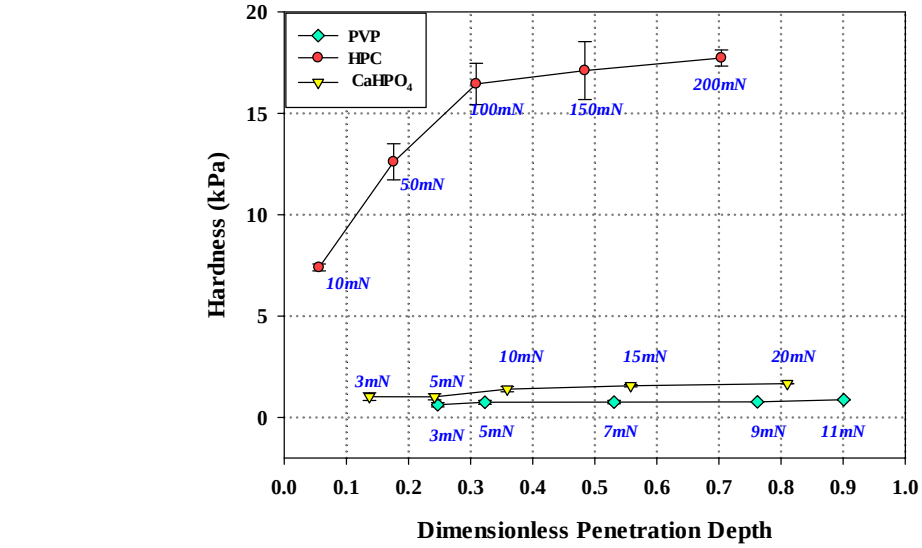

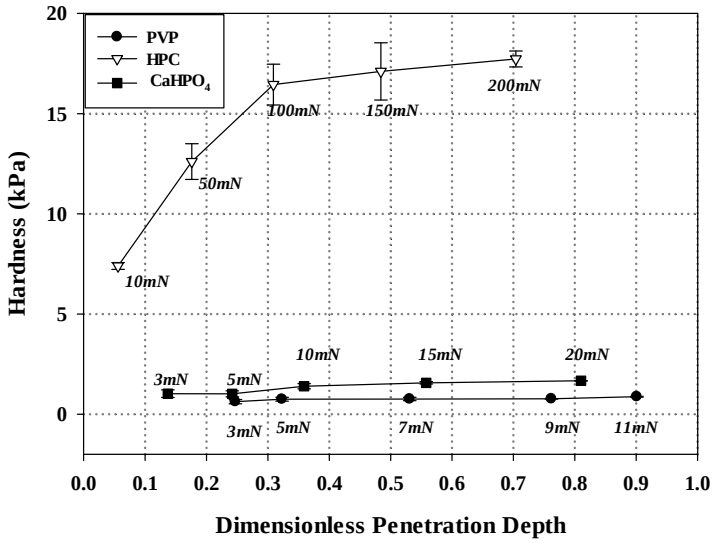

Figure 5 b) (Colour; Black and white)

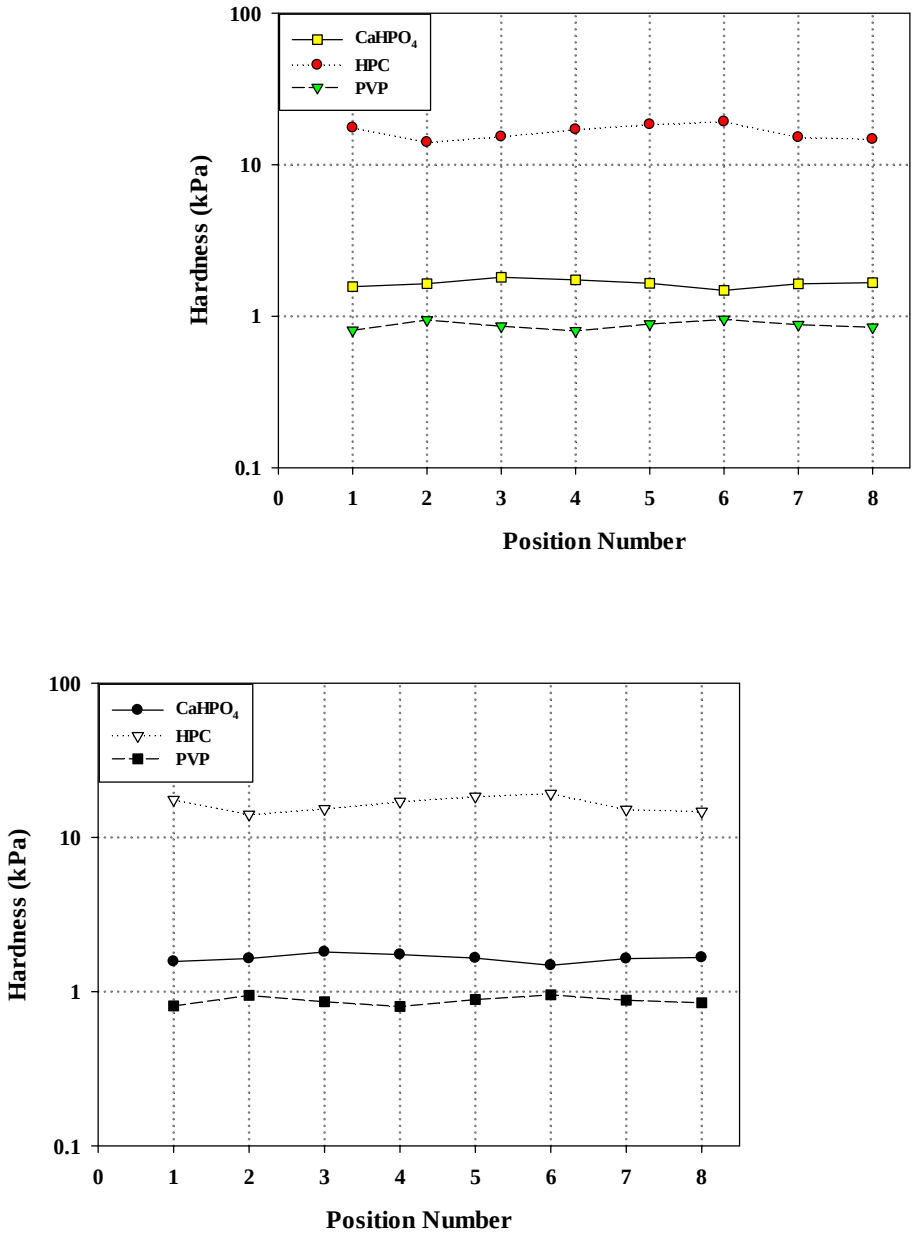

Figure 5. Effect of indentation load (a) and position (b) on the hardness of powder beds of test materials

Figure 6

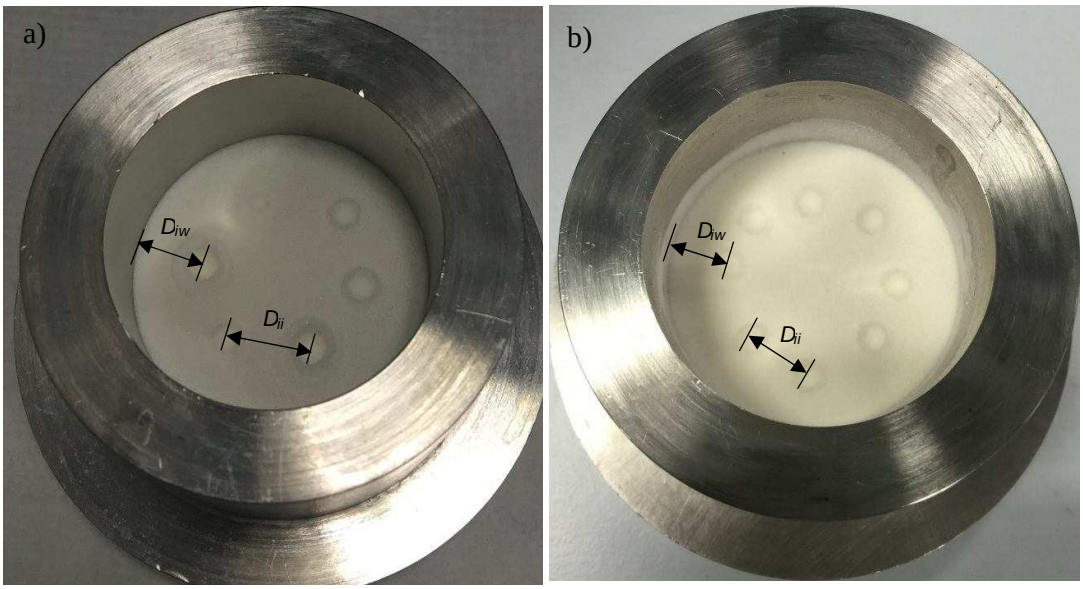

Figure 6. The photos of ball indentation experiments at different indentation loads (a), and positions (b)

Figure 7 a) (Colour; Black and white)

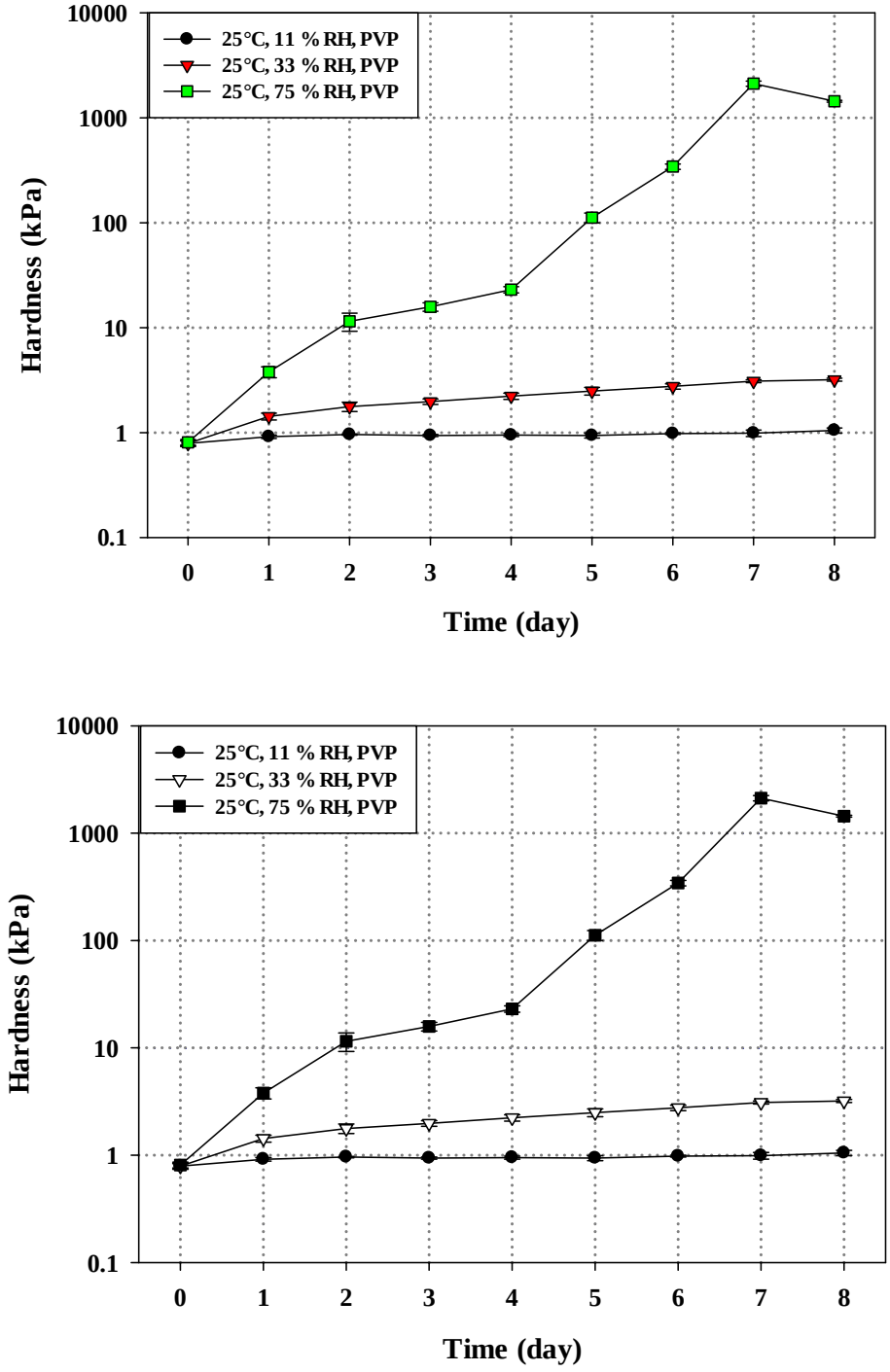

Figure 7 b) (Colour; Black and white)

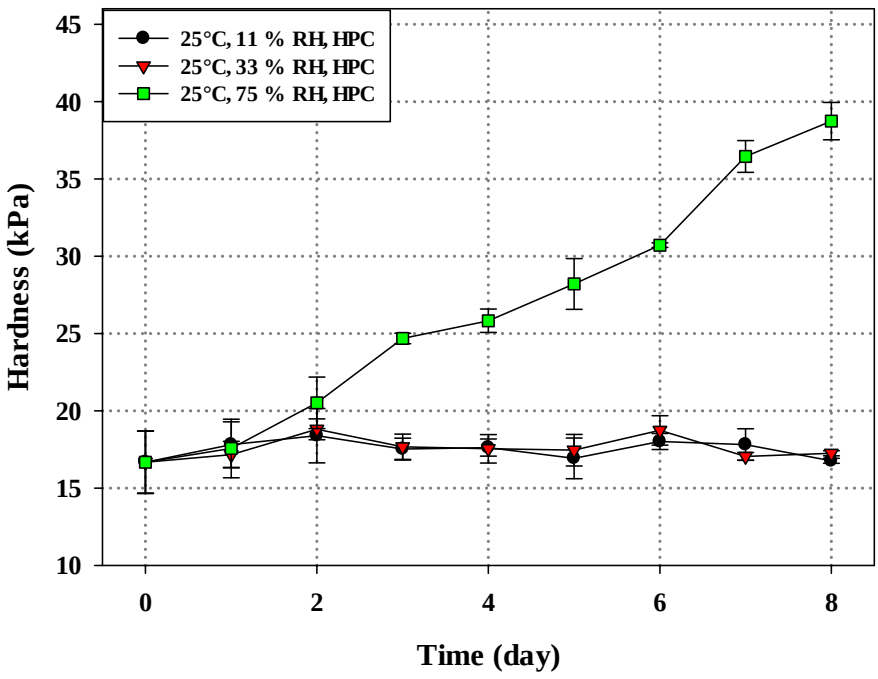

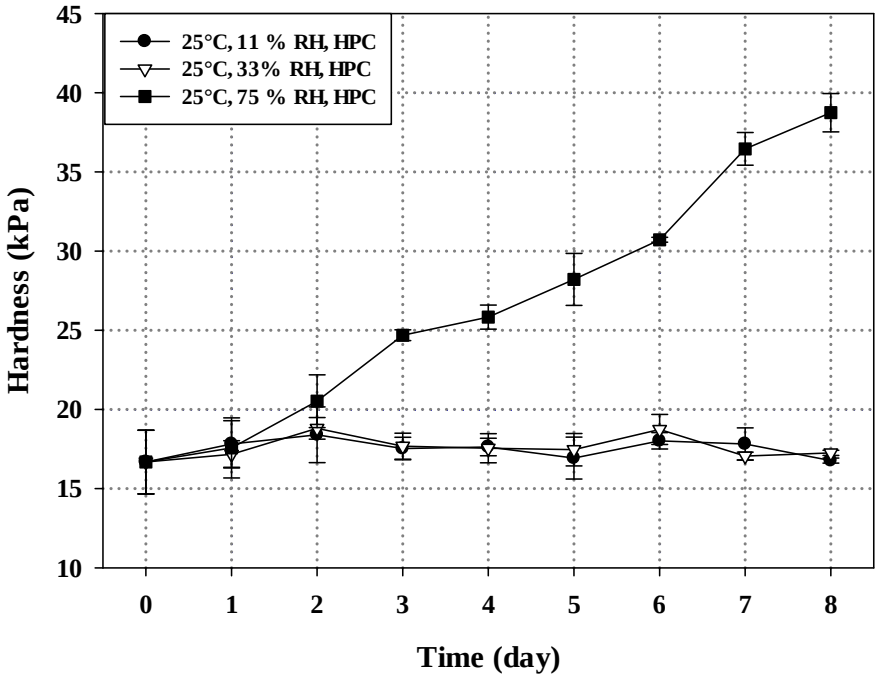

Figure 7 c) (Colour; Black and white)

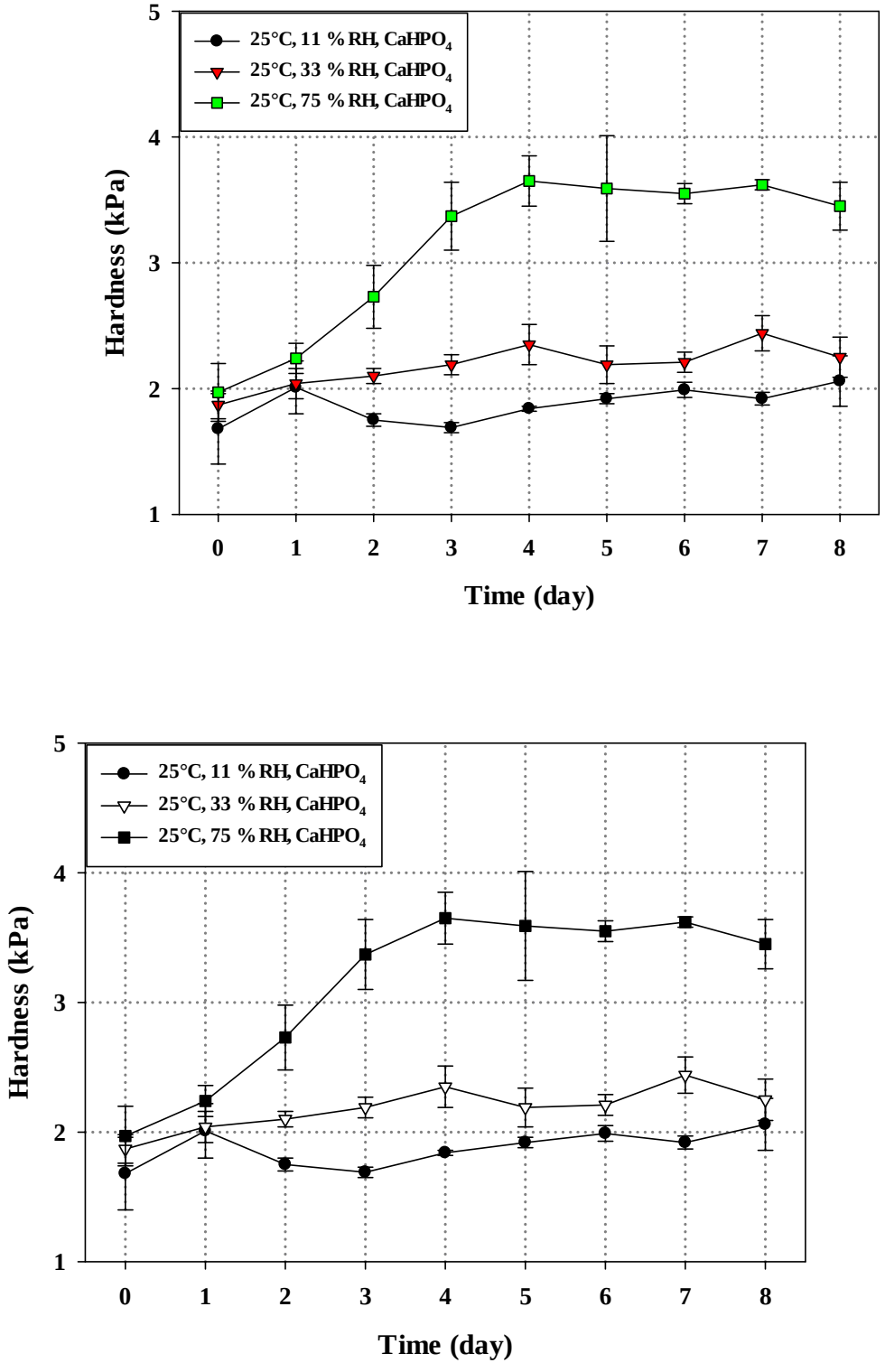

Figure 7. Effect of relative humidity on the surface hardness of (a) PVP, (b) HPC and (c) $CaHPO_4$ at 25 °C

Figure 8 (Colour; Black and white)

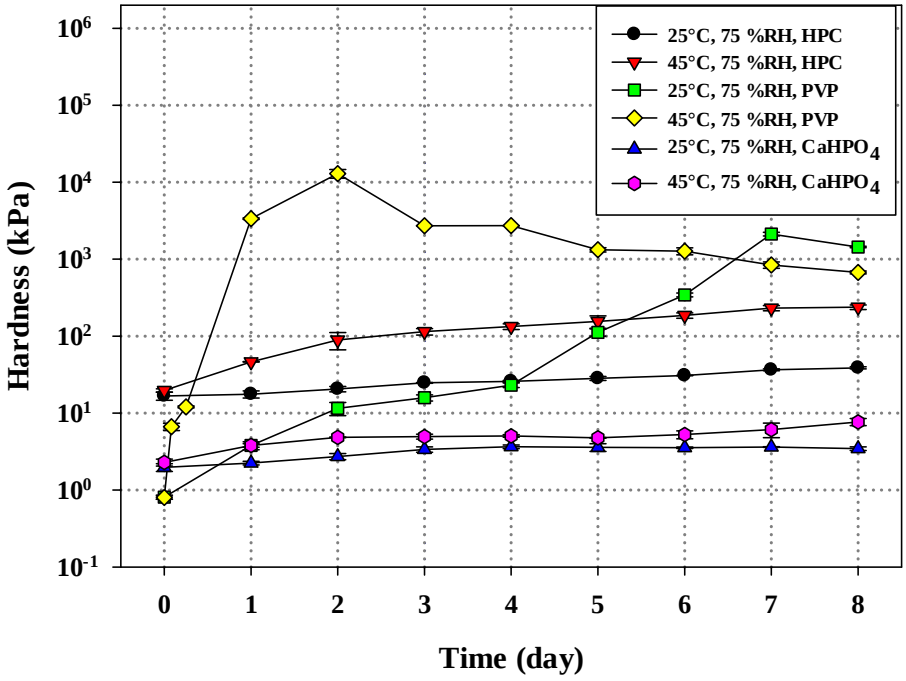

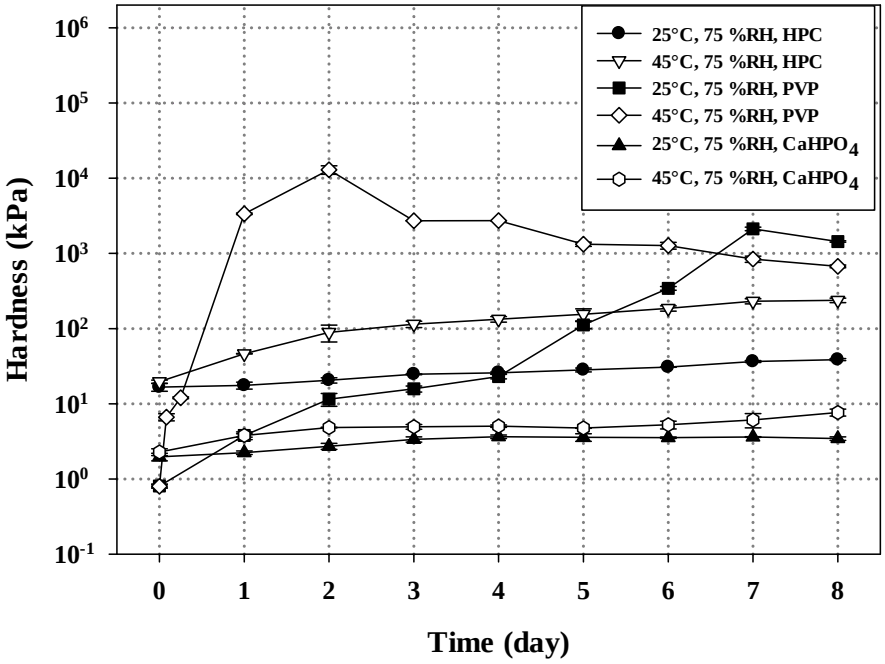

8. Effect of temperature at constant RH on the surface hardness of powder beds of HPC, PVP and $CaHPO_4$

Figure 9. Relative humidity (RH) ramping experiment (10%RH/h) for PVP at 25 °C. Red line shows the net change in mass while the blue line shows the RH profile of sample

Figure 9 (Colour)

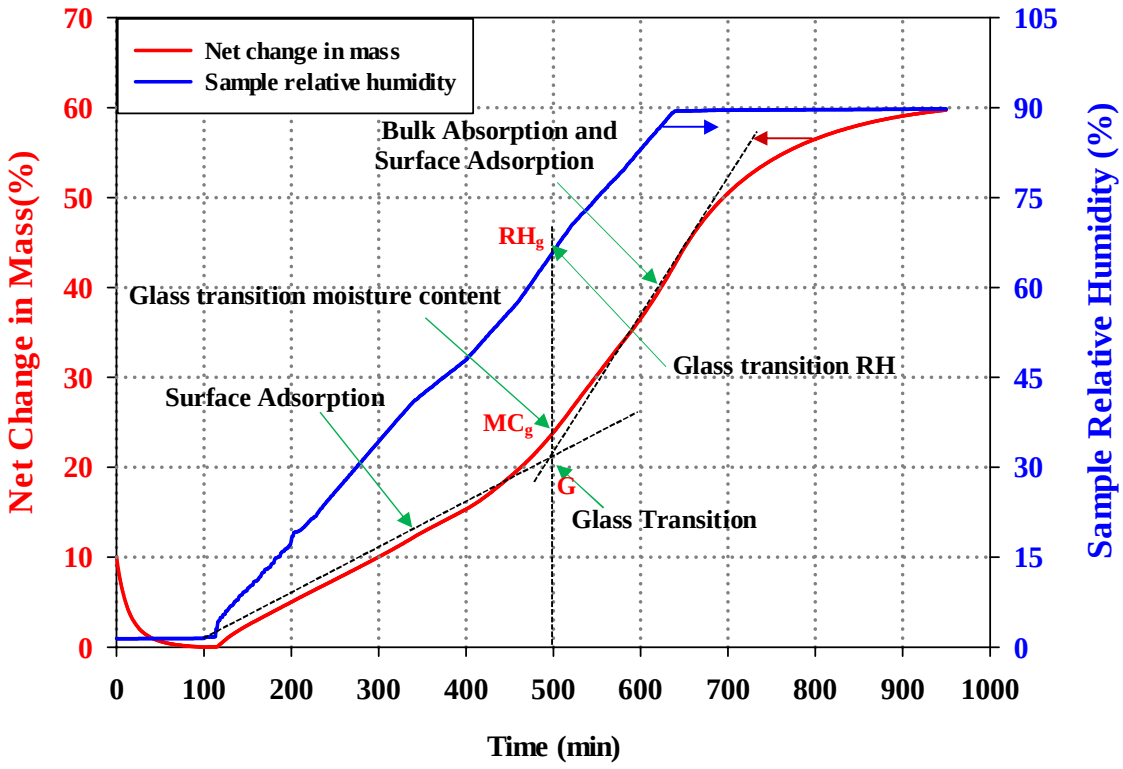

Figure 9 (Black and white)

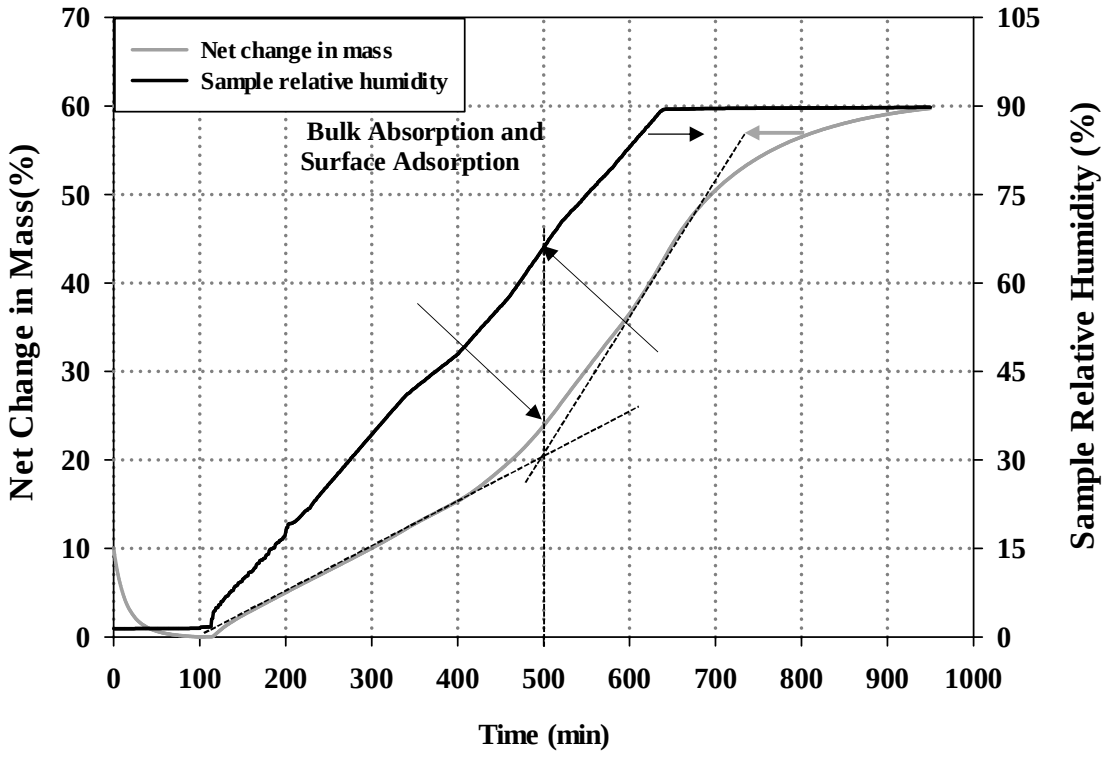

Figure 10 (Colour)

a)

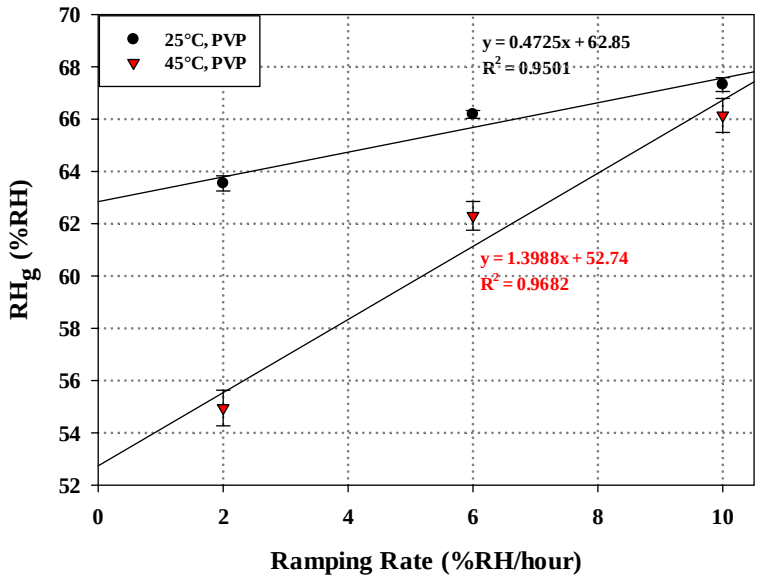

b)

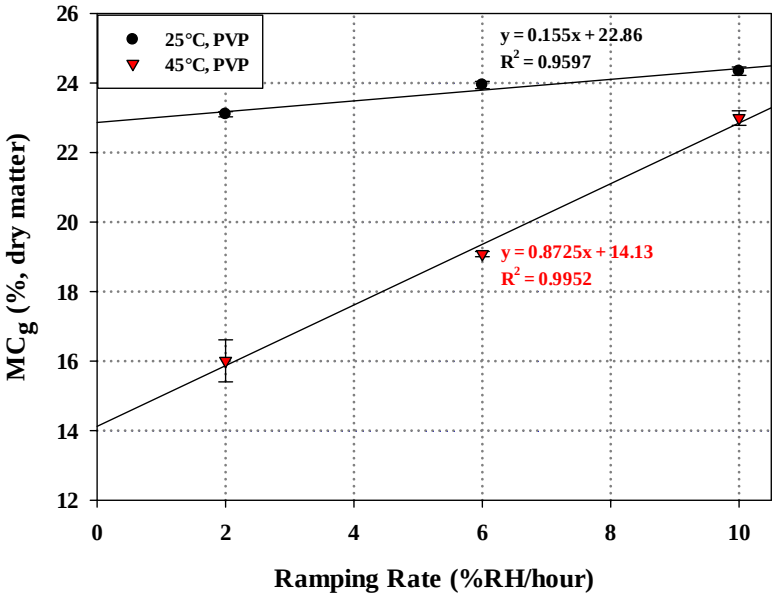

Figure 10 (Colour)

a)

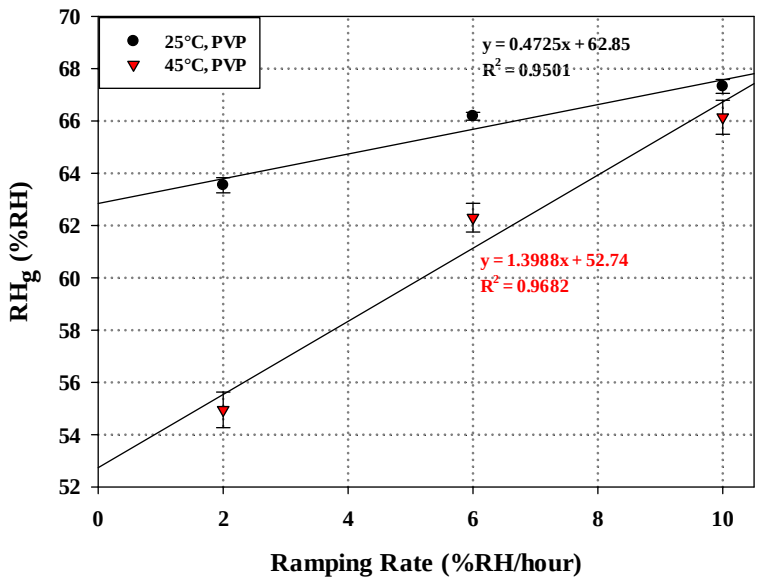

b)

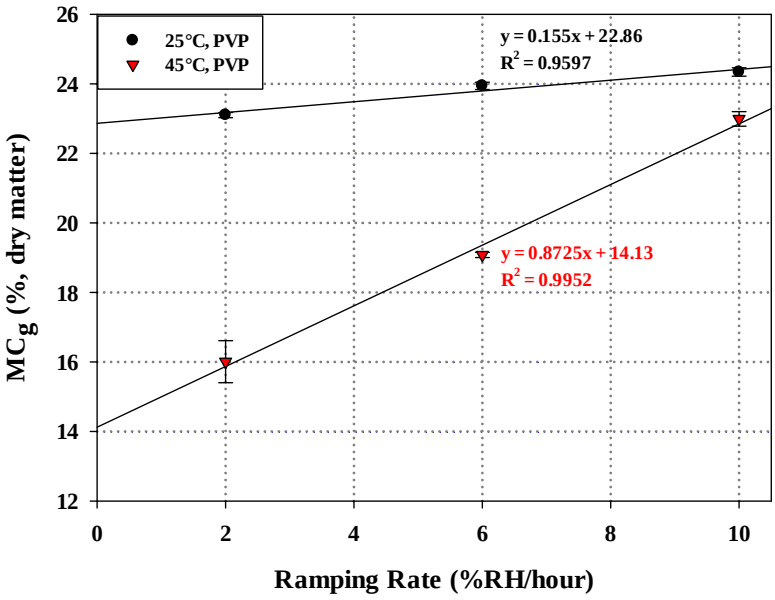

Figure 10 (Black and white)

a)

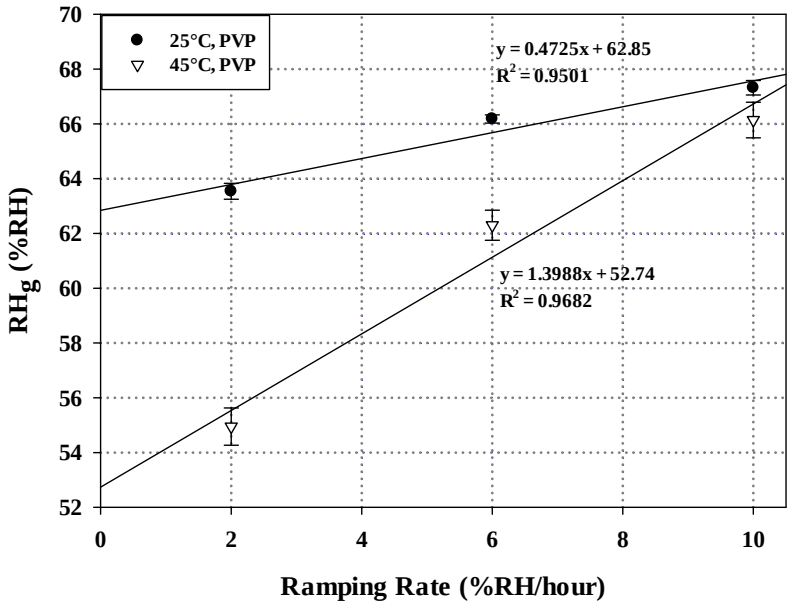

b)

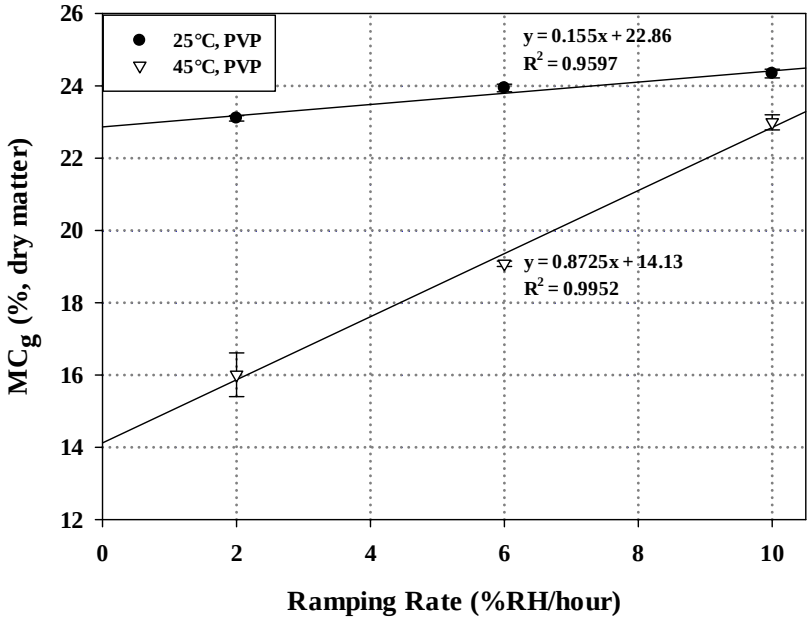

Figure 10. (a) Glass transition relative humidity and (b) glass transition moisture content as a function of the ramping rate for PVP at 25 °C and 45 °C. Solid line and equation represent the linear fit

Figure 10 (Colour)

a)

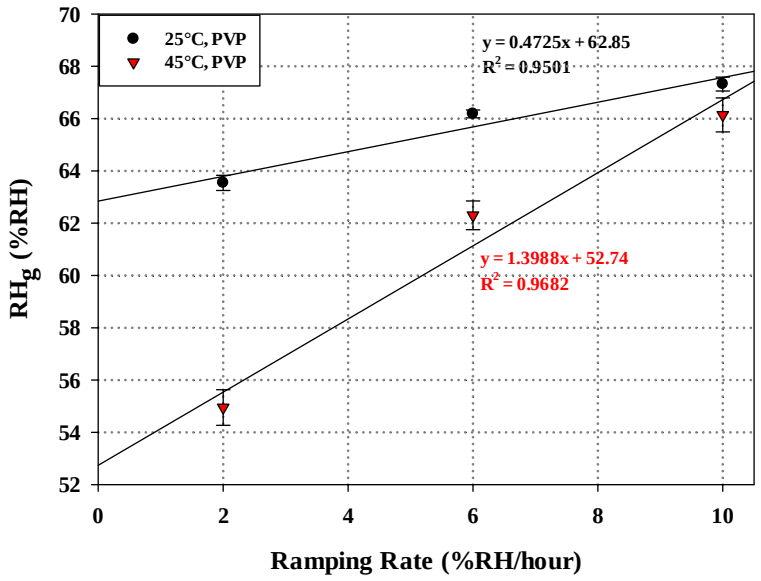

b)

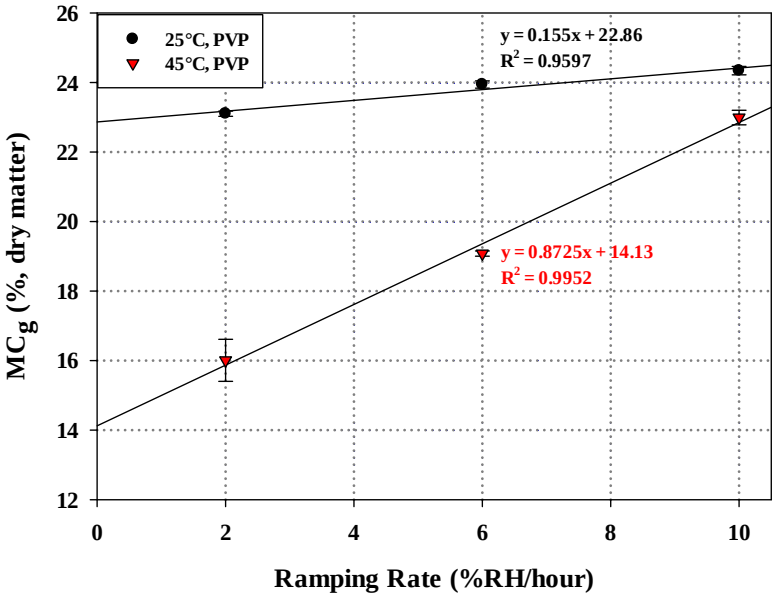

Figure 10 (Black and white)

a)

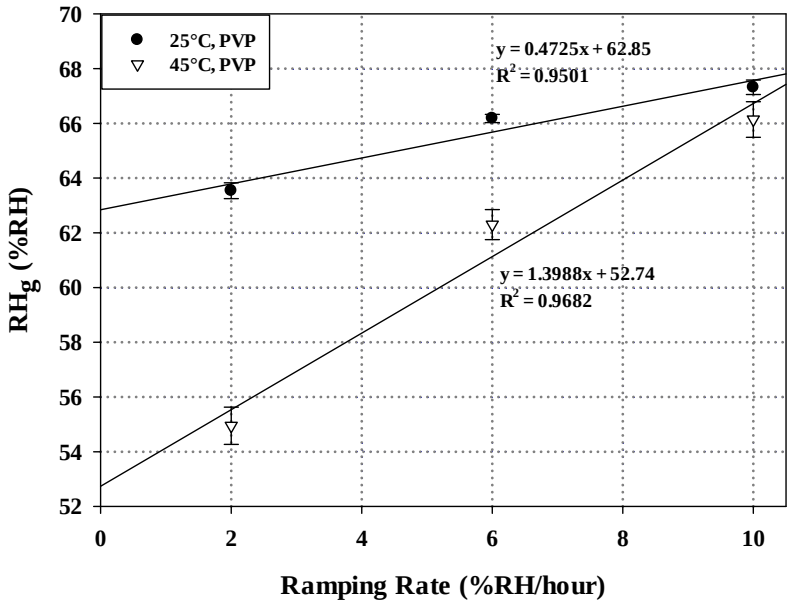

b)

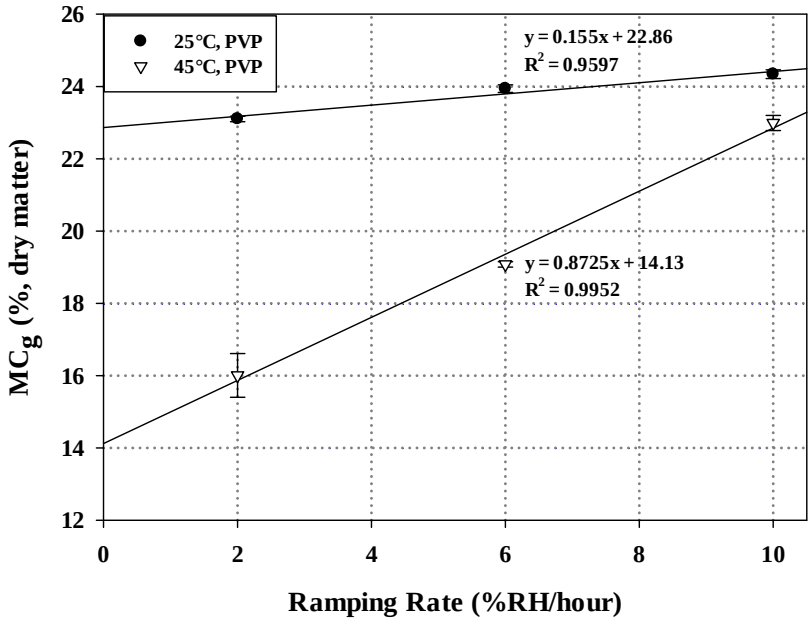

Figure 11 a) 25 °C (Colour; Black and white)

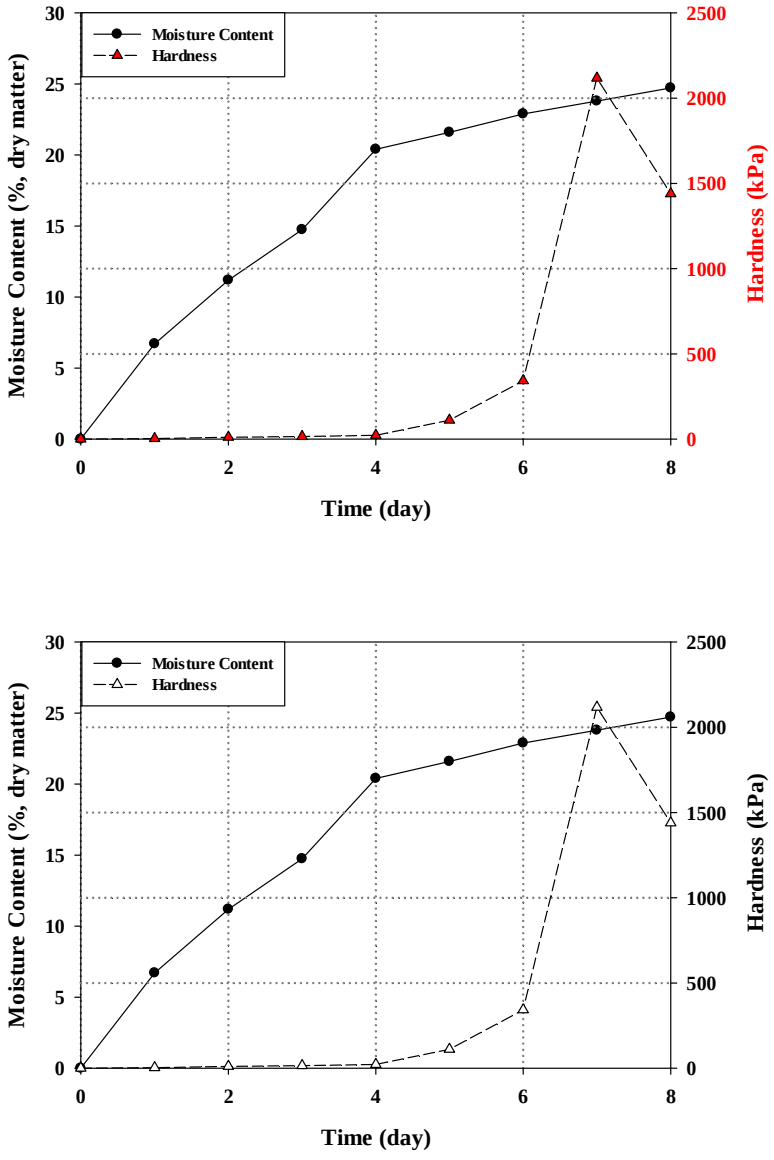

Figure 10 (Colour)

a)

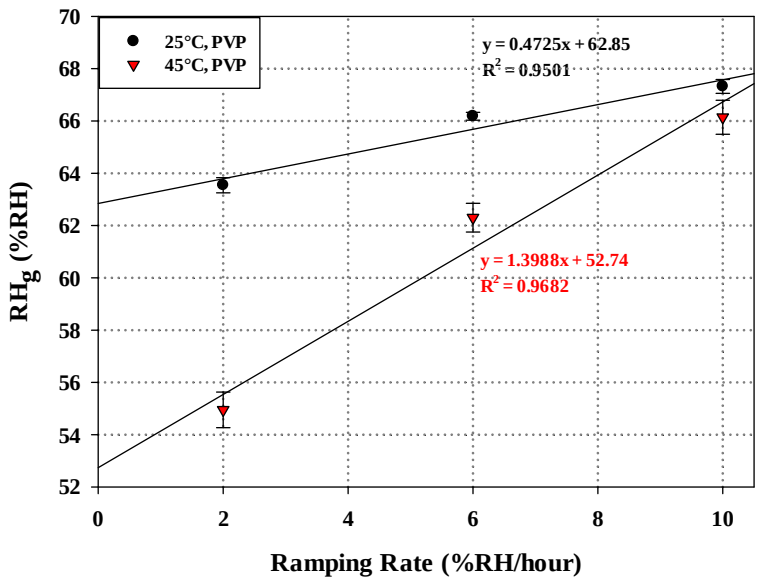

b)

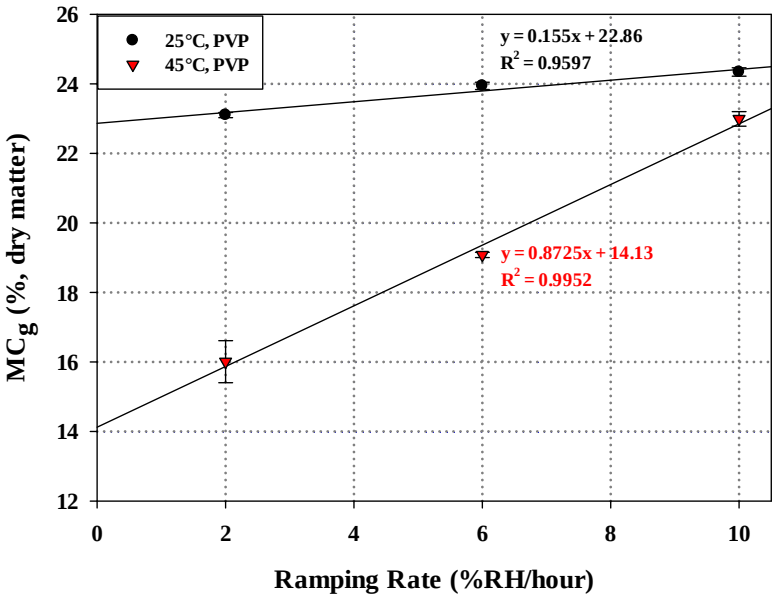

Figure 10 (Black and white)

a)

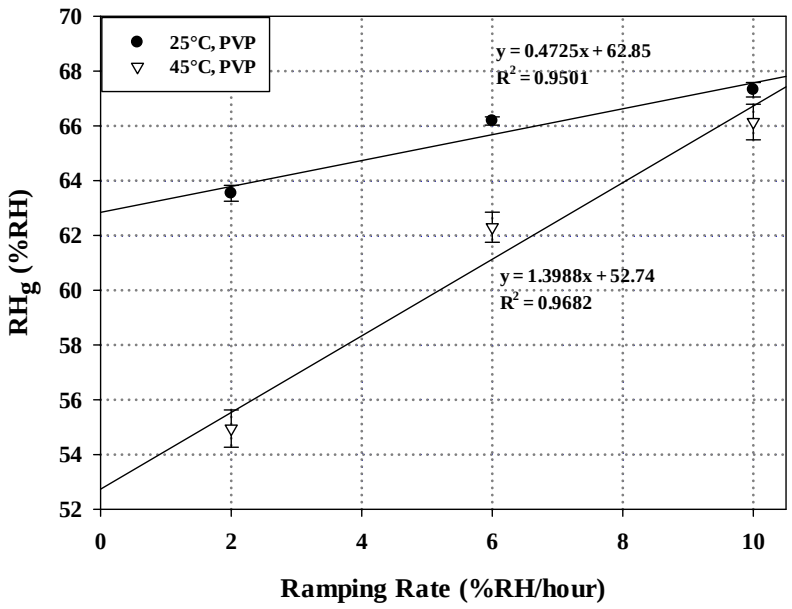

b)

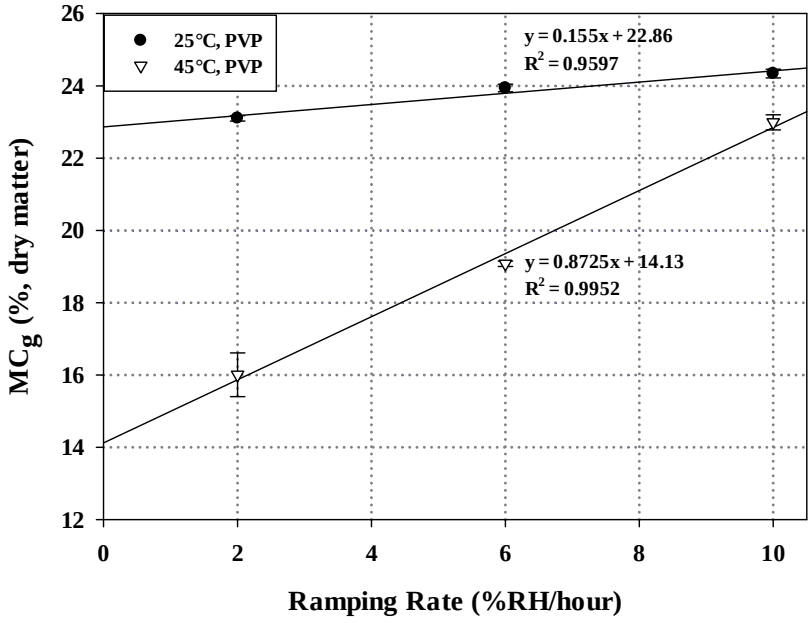

Figure 11 a) 25 °C (Colour; Black and white)

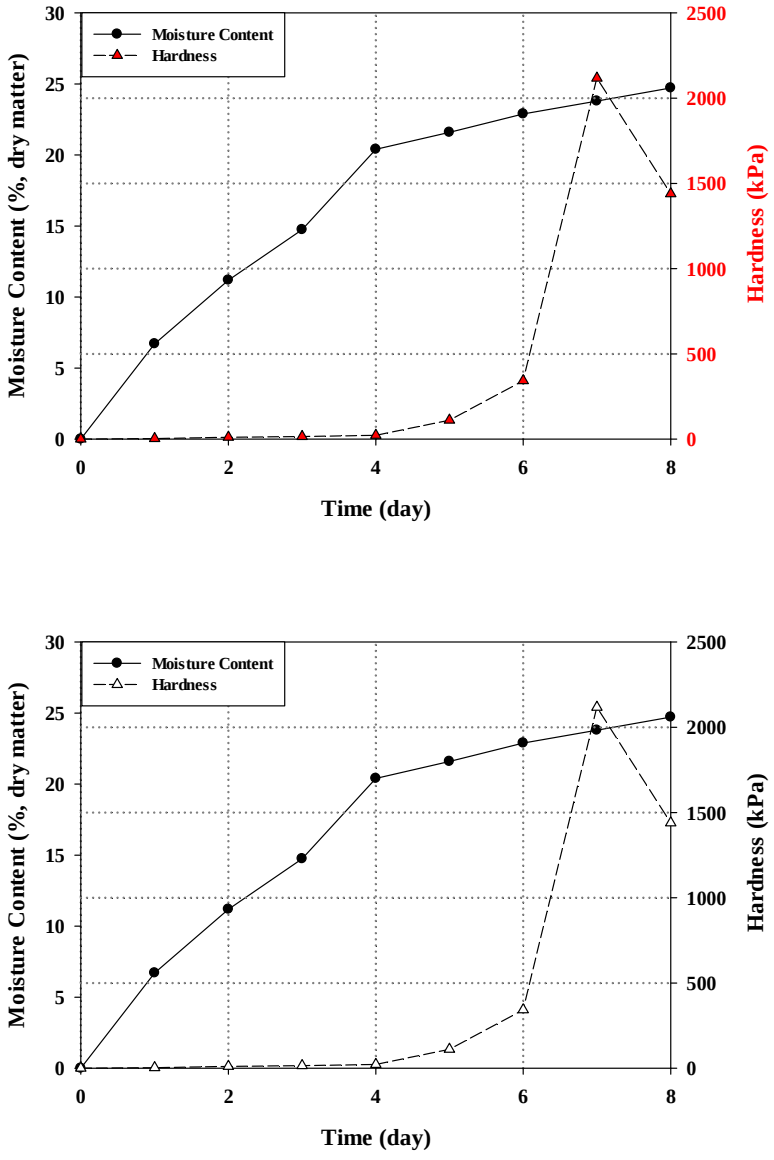

Figure 11 b) 45 °C (Colour; Black and white)

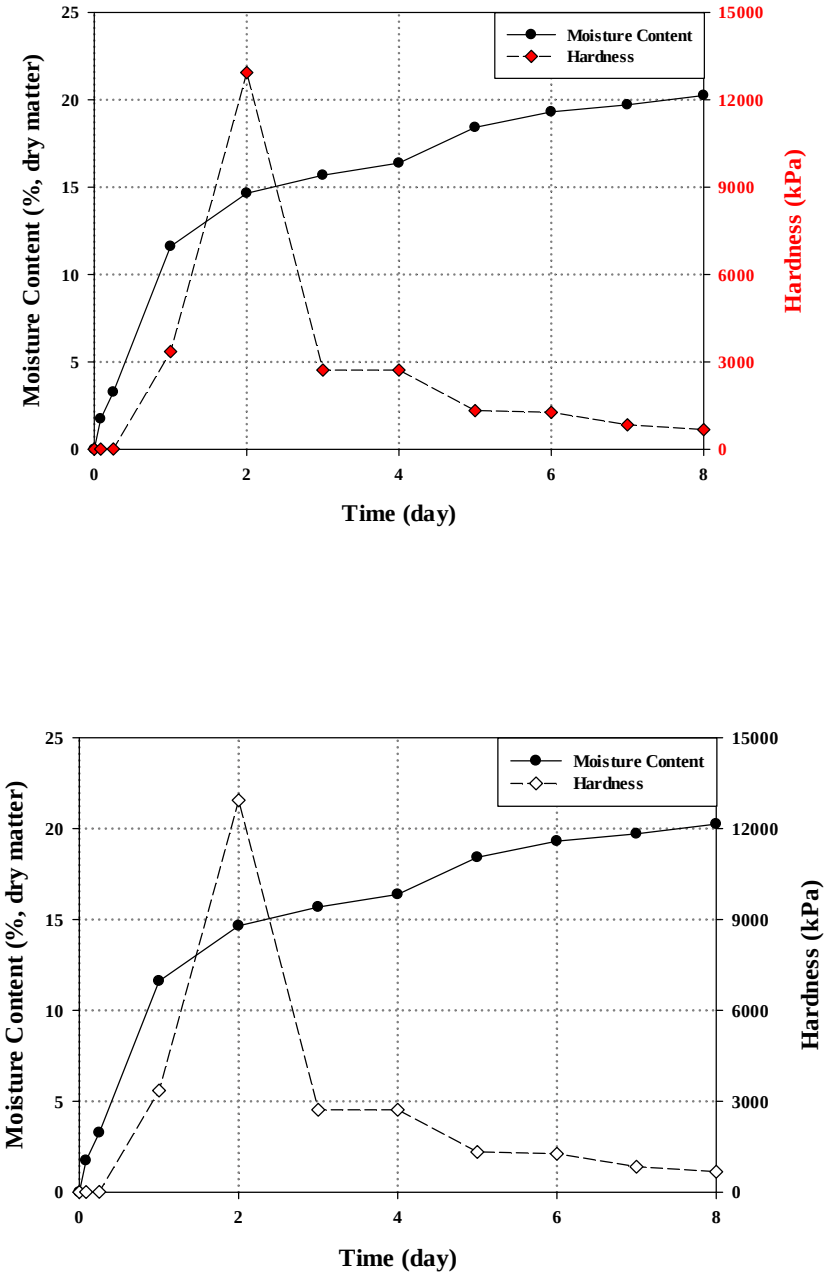

Figure 11. Moisture uptake and hardness change of PVP as a function of time at (a) 25 °C and (b) 45 °C

Figure 10 (Colour)

a)

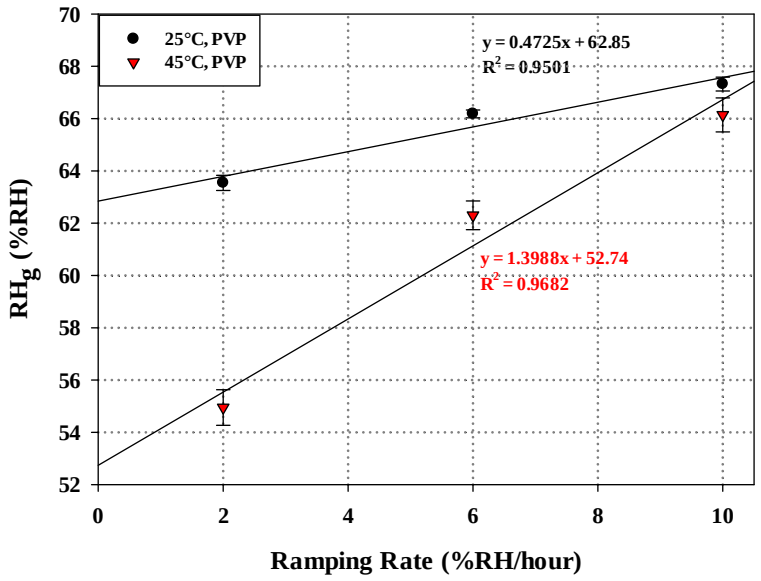

b)

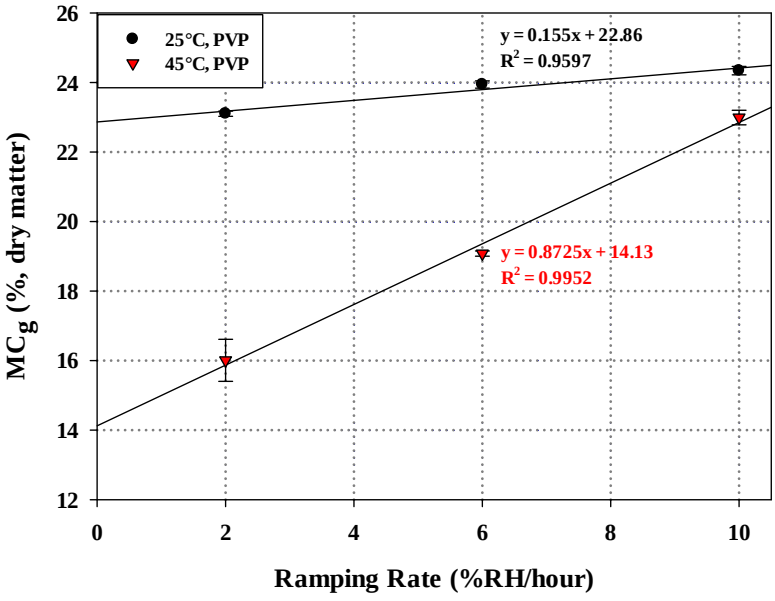

Figure 10 (Black and white)

a)

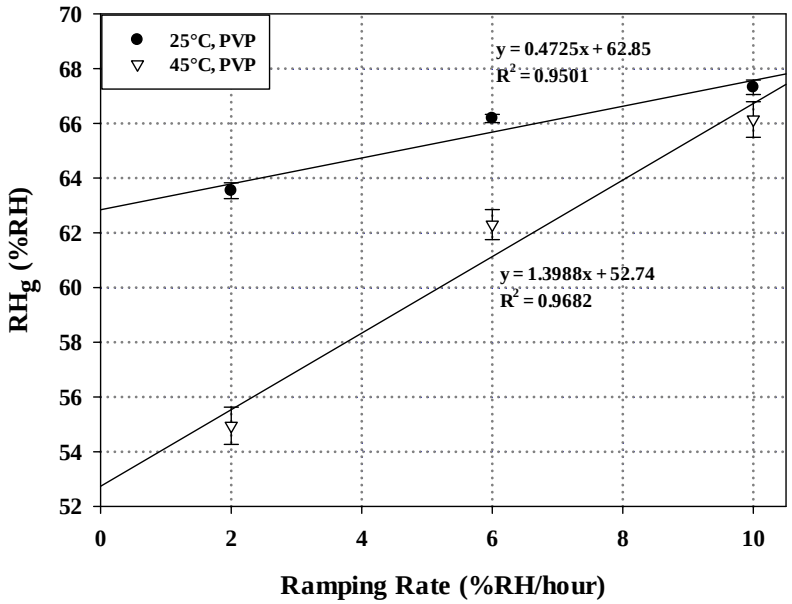

b)

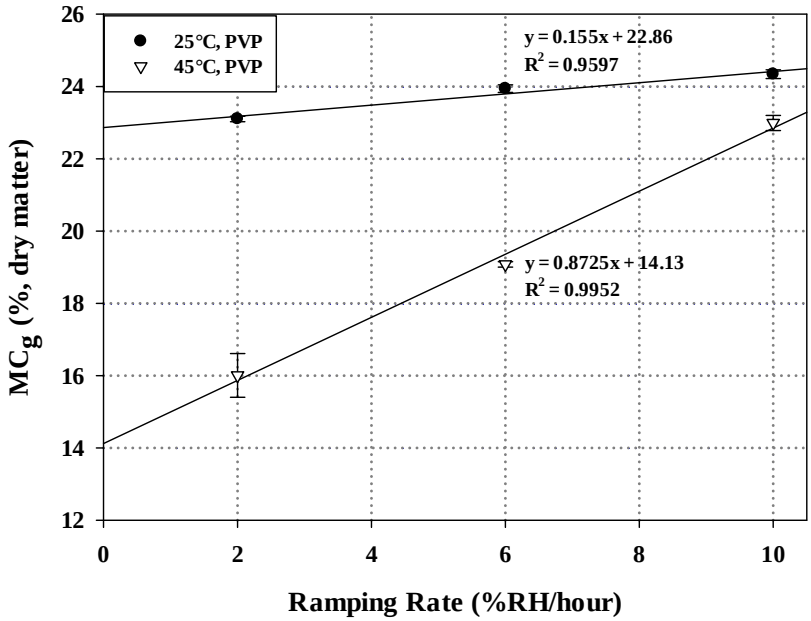

Figure 11 a) 25 °C (Colour; Black and white)

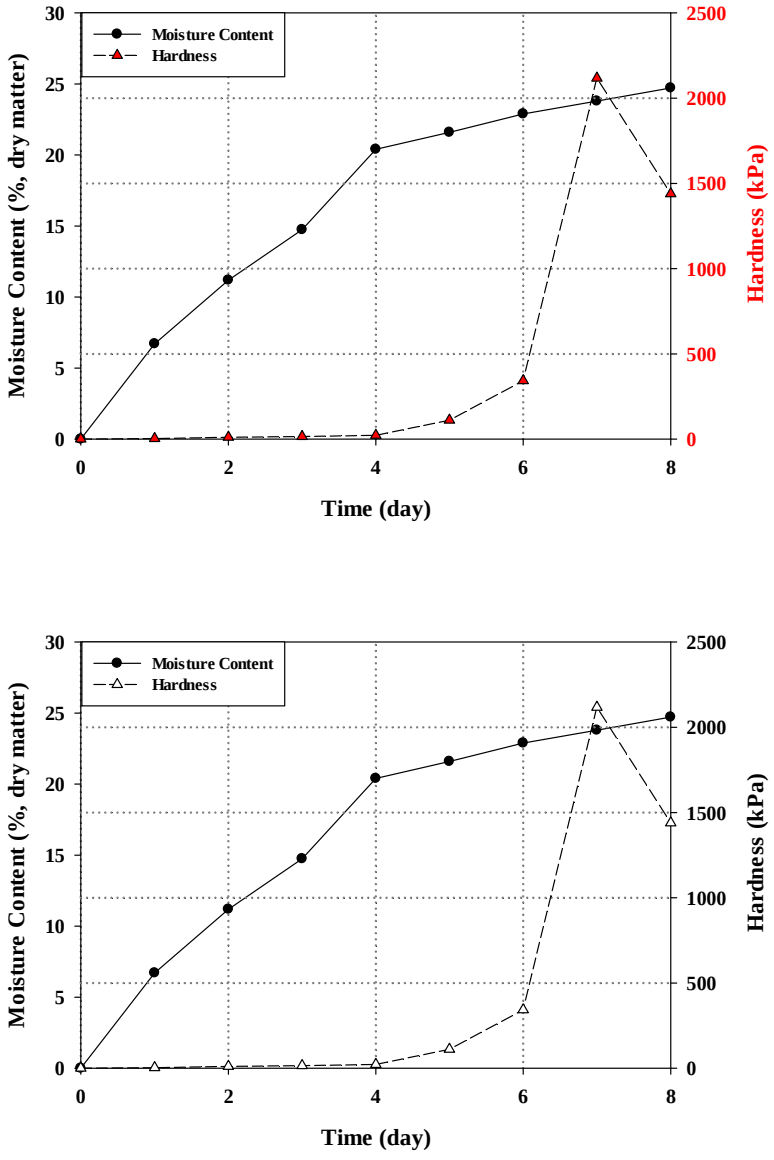

Figure 11 b) 45 °C (Colour; Black and white)

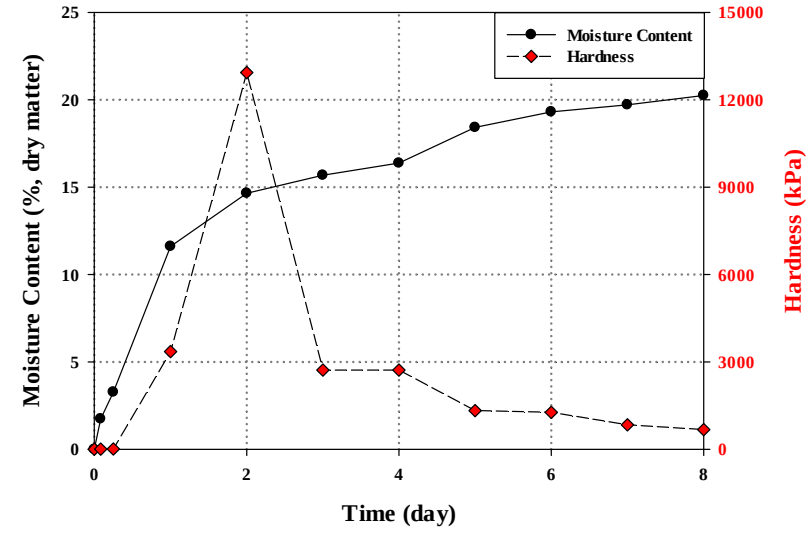

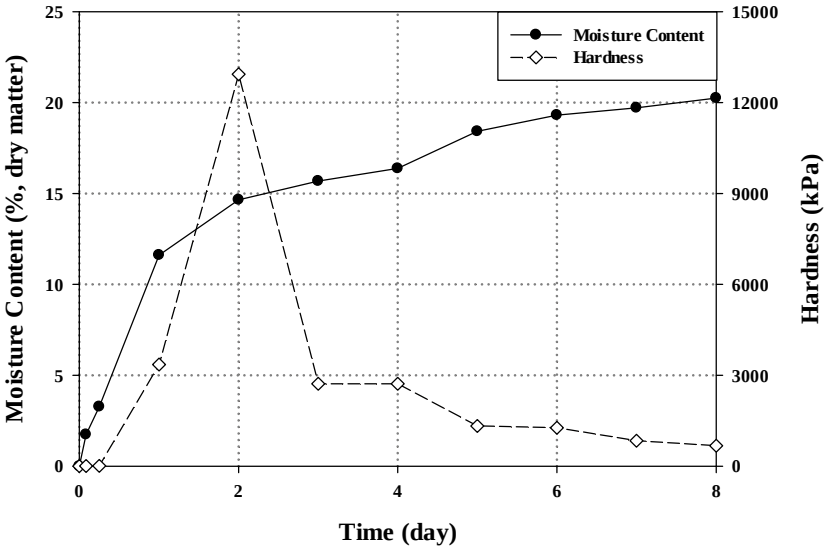

Figure 12 (Colour; Black and white)

a)

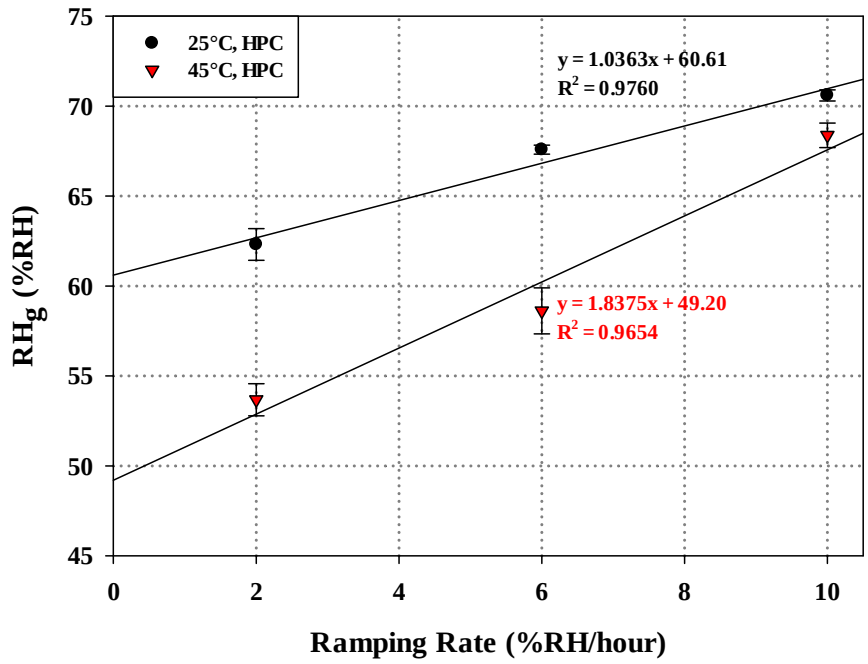

b)

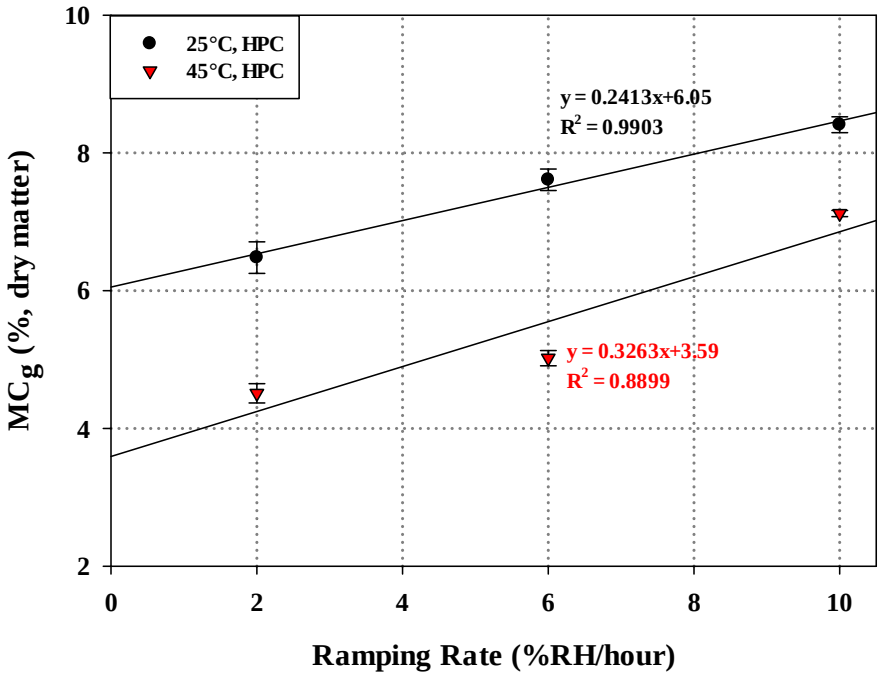

Figure 12 (Black and white)

a)

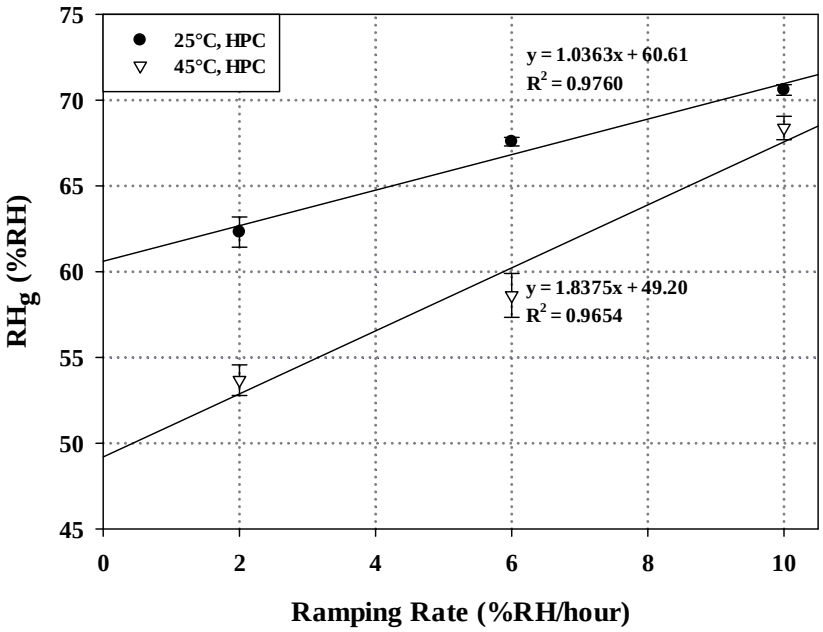

b)

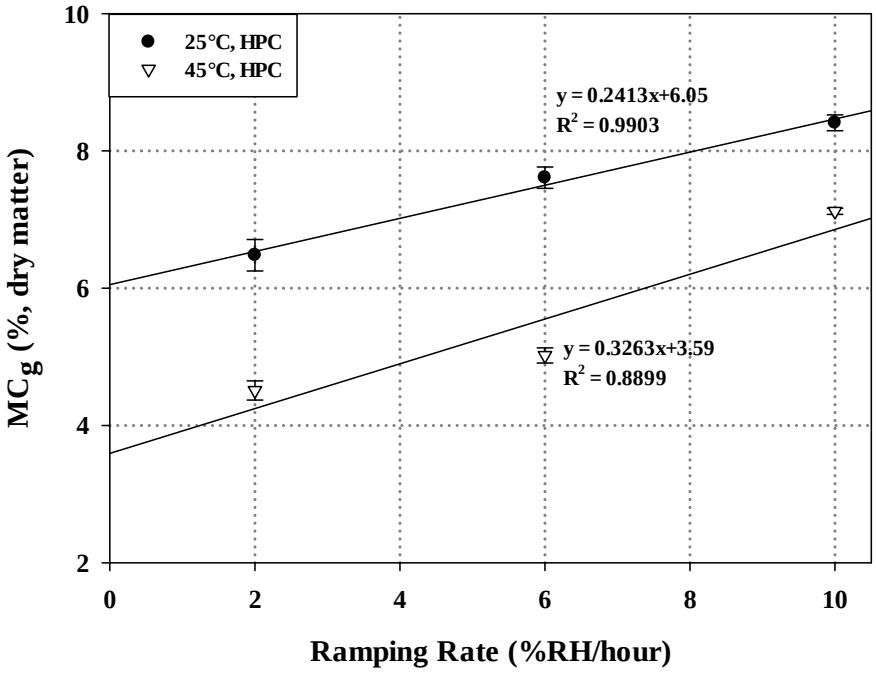

Figure 12. (a) Glass transition relative humidity and (b) glass transition moisture content as a function of

ramping rate for HPC at 25 °C and 45 °C. Solid line and equation represent the linear fit

Figure 12 (Black and white)

a)

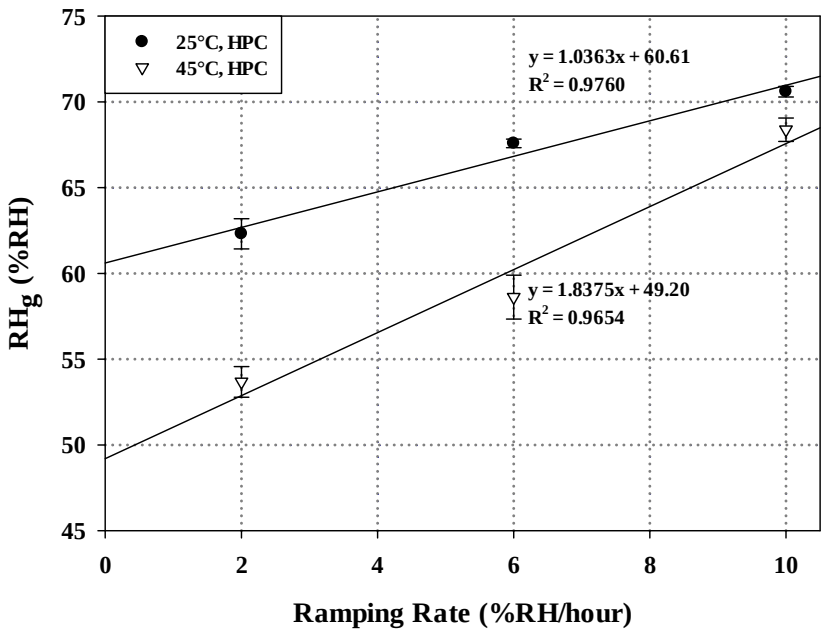

b)

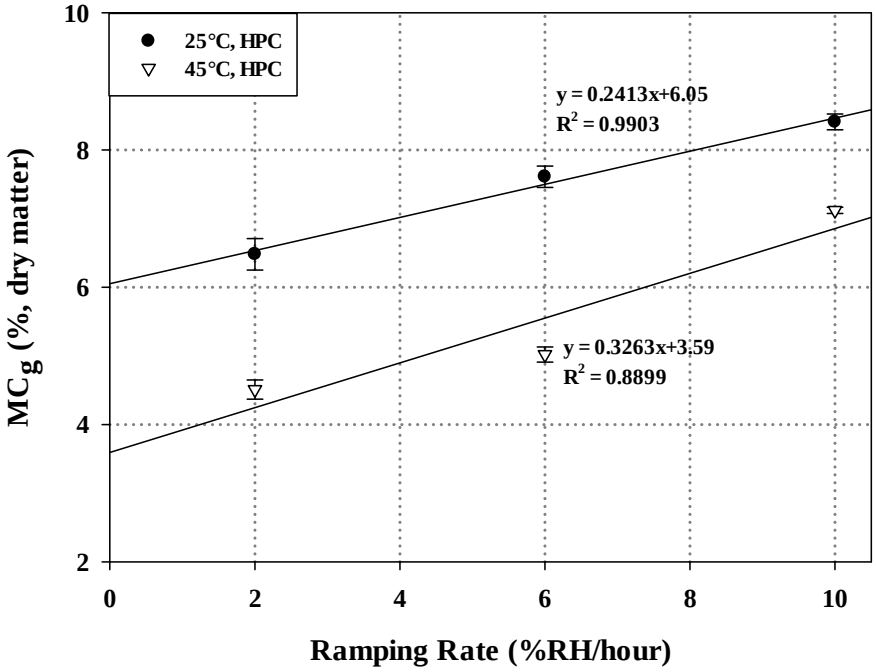

Figure 13 a) 25 °C (Colour; Black and white)

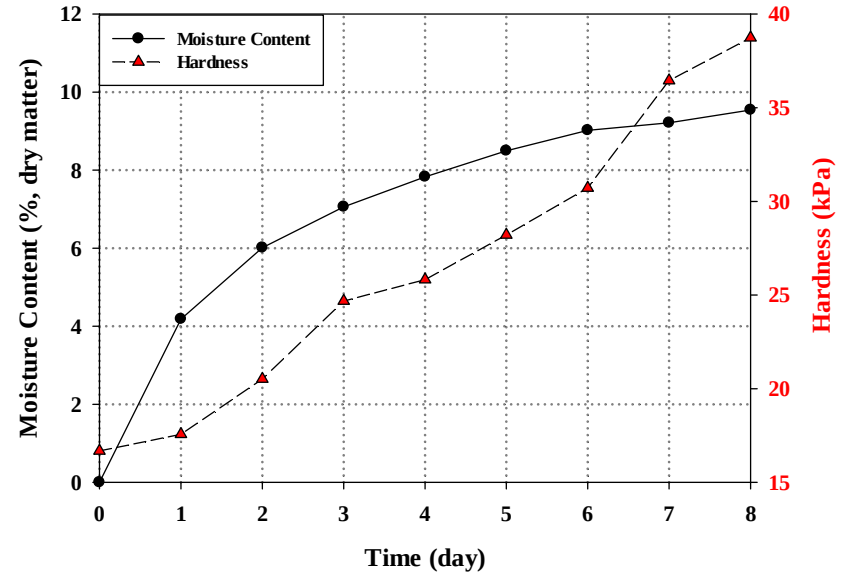

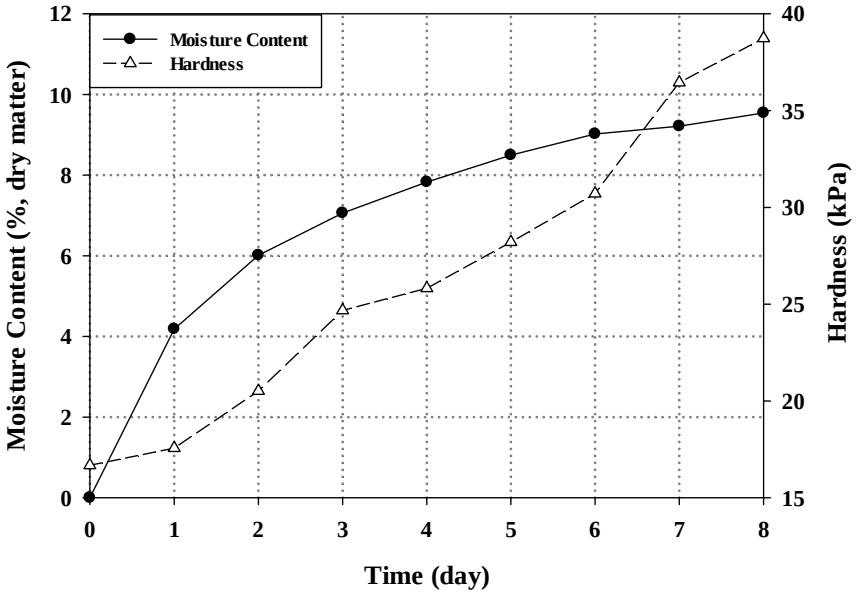

Figure 12 (Black and white)

a)

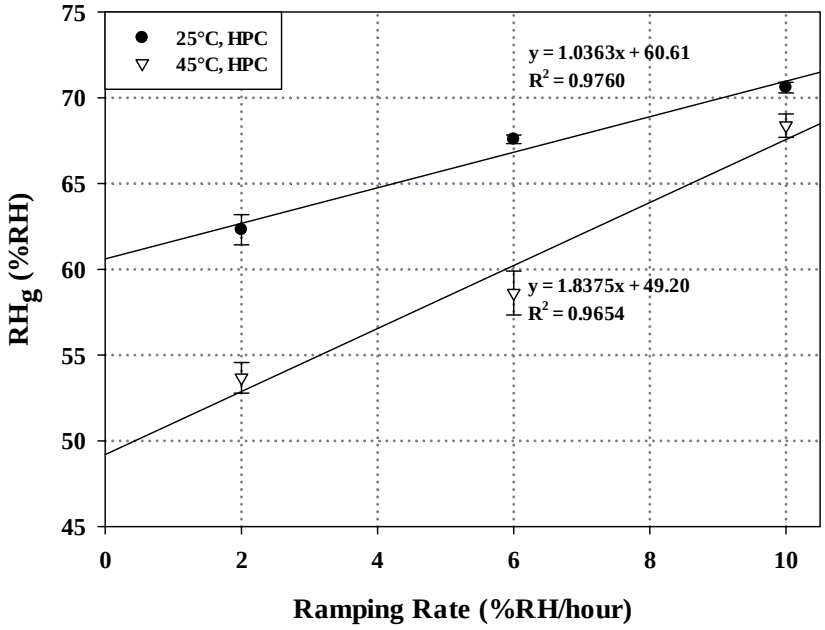

b)

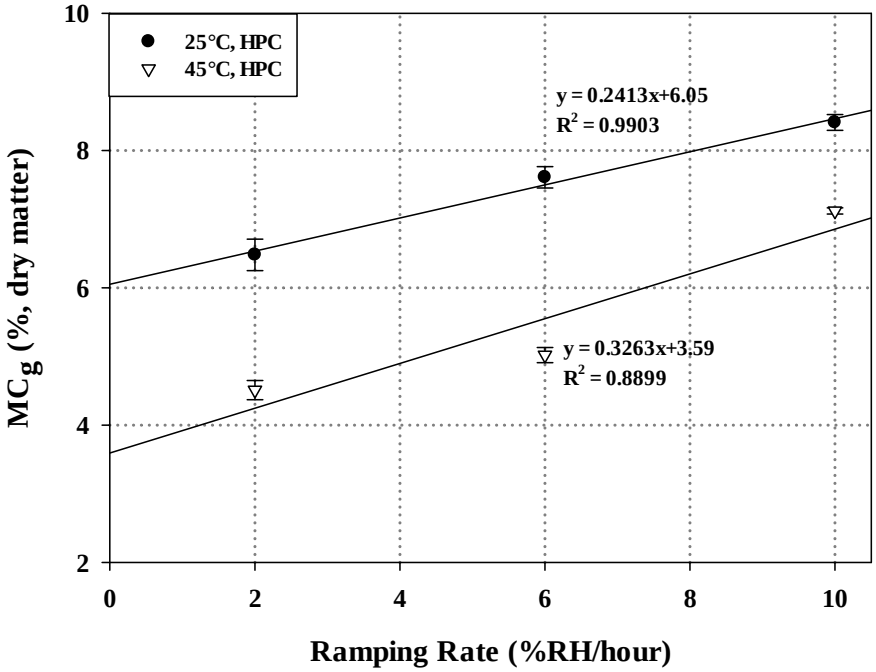

Figure 13 a) 25 °C (Colour; Black and white)

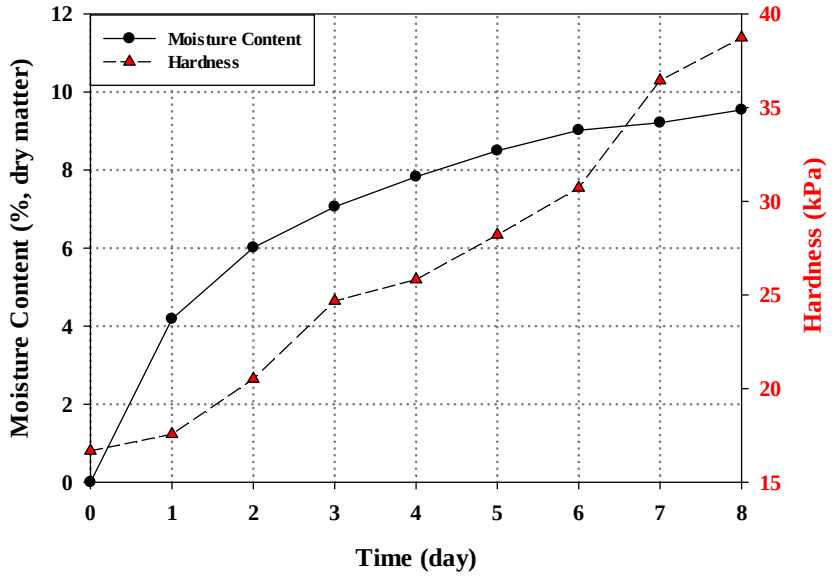

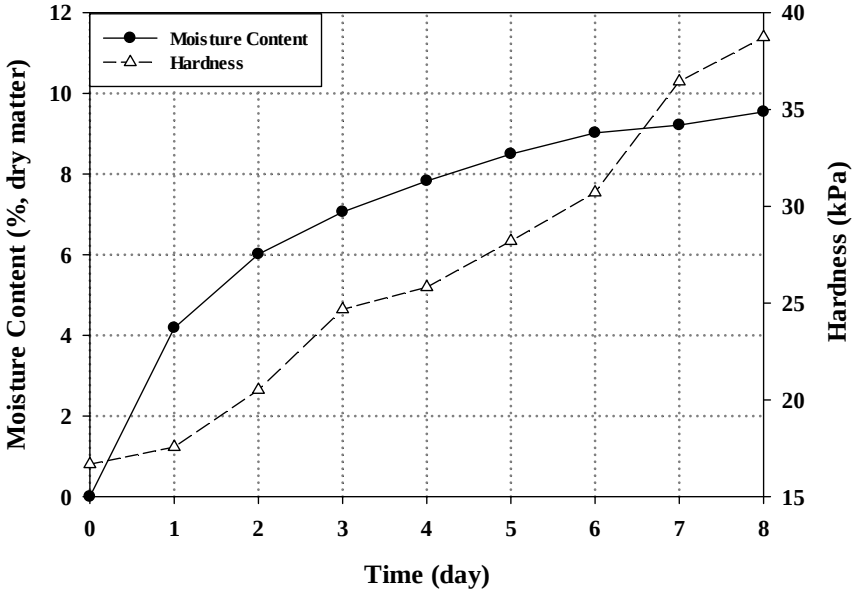

Figure 13 b) 45 °C (Colour; Black and white)

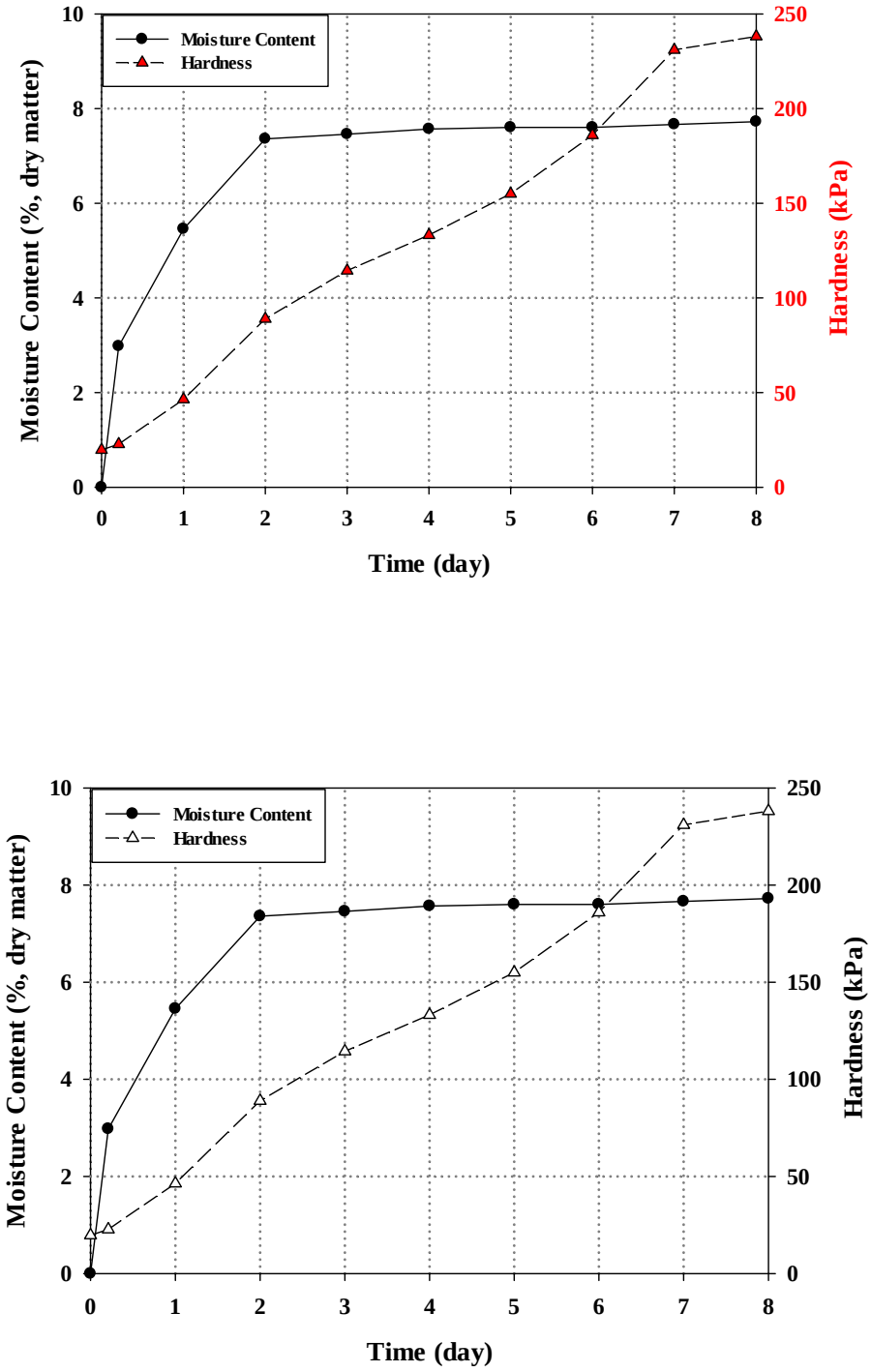

Figure 13. Moisture uptake and hardness change of HPC as a function of time at (a) 25 °C and (b) 45 °C

Table 1. Size and shape parameters of test powders

Parameters	PVP	HPC	$CaHPO_4$
CE $D_{[v,0.1]}$ (µm)	38±3	33±2	75±8
CE $D_{[v,0.5]}$ (µm)	81±10	81±3	197±9
CE $D_{[v,0.9]}$ (µm)	135±14	130±20	292±10
Circularity	0.969 ±0.005	0.666±0.002	0.779±0.003
Aspect Ratio	0.934±0.005	0.552±0.010	0.671±0.001
Elongation	0.066±0.005	0.448±0.010	0.329±0.001